

AD-A205 519

REPORT DOCUMENTATION PAGE		READ INSTRUCTIONS BEFORE COMPLETING FORM
1. REPORT NUMBER R/D 5027-OH-01	2. GOVT ACCESSION NO.	3. RECIPIENT'S CATALOG NUMBER
4. TITLE (and Subtitle) COLLOIDAL ASSEMBLIES EFFECT ON CHEMICAL REACTIONS	5. TYPE OF REPORT & PERIOD COVERED FINAL AUGUST 1985 - DECEMBER 88	
7. AUTHOR(s) Ezio PELIZZETTI	8. CONTRACT OR GRANT NUMBER(s) DAJA 45-85-C-0023	
9. PERFORMING ORGANIZATION NAME AND ADDRESS Università di Torino Via Verdi 8, 10125 Torino, Italy	10. PROGRAM ELEMENT, PROJECT, TASK AREA & WORK UNIT NUMBERS	
11. CONTROLLING OFFICE NAME AND ADDRESS	12. REPORT DATE DECEMBER 1988	
	13. NUMBER OF PAGES 29	
MONITORING AGENCY NAME & ADDRESS (if different from Controlling Office)	15. SECURITY CLASS. (of this report)	
	15a. DECLASSIFICATION/DOWNGRADING SCHEDULE	
DISTRIBUTION STATEMENT (of this Report) PROVED FOR PUBLIC RELEASE - DISTRIBUTION UNLIMITED		
DISTRIBUTION STATEMENT (of the abstract entered in Block 20, if different from Report)		
16. SUPPLEMENTARY NOTES		
19. KEY WORDS (Continue on reverse side if necessary and identify by block number) COLOIDS } MICELLES } MICROEMULSIONS } SURFACTANTS } OXIDATION } PHOTOCATALYSIS } SEMICONDUCTORS } DEGRADATION } MINERALIZATION } HALOAROMATIC COMPOUNDS } REACTION MECHANISMS } KINETICS. <i>signature</i> ←		
20. ABSTRACT (Continue on reverse side if necessary and identify by block number) The influence that organized assemblies (micelles, microemulsions) and semiconductor colloids exhibits on chemical reactions has been investigated. In particular electron transfer reactions induced by light in the presence of semiconductor particles have been shown to completely degrade potentially dangerous compounds.		

DD FORM 1 JAN 73 1473 EDITION OF 1 NOV 65 IS OBSOLETE

SECURITY CLASSIFICATION OF THIS PAGE (When Data Entered)

89 2 22 043

The photodegradation catalyzed by TiO_2 particles of phenol, p-alkylphenols and ethoxylated non-ionic surfactants derived from p-nonylphenol has been investigated by carrying out the experiments in different experimental conditions. Intermediate formation has been followed through HPLC analysis. CO_2 evolution as well as DOC and POC measurements confirm the complete degradation.

Similarly, the photocatalytic degradation of 2,4,5-trichlorophenoxyacetic acid (2,4,5-T) and 2,4,5-trichlorophenol on TiO_2 led to complete mineralization into CO_2 and HCl . In the degradation of 2,4,5-T several intermediates were detected by GC-MS and a scheme for the photodegradation pathways was formulated.

The photodegradation process in the presence of semiconductors has been shown to be efficient also with persistent and sparingly soluble haloaromatic compounds such as DDT, dioxins, PCB's. The photoreactions at semiconductors of some non-halogenated solvents, i.e. cellosolves, have been shown to effectively degrade also these water-miscible contaminants.

Finally, herbicides of the s-triazine family (e.g. atrazine) have been degraded even at ppb levels.

Since the proposed photodegradative mechanism involves the intervention of OH^\cdot radicals, Fenton's reagent ($\text{Fe}^{2+} + \text{H}_2\text{O}_2$) was investigated as possible reagent for halophenols degradation. The mineralization of these compounds was, in fact, found to occur and the effect of the concentration of Fe^{2+} , Fe^{3+} , HClO_4 was investigated.

Microemulsions are transparent dispersion of oil-in-water (O/W) or water-in-oil (W/O) in the presence of a surfactant and a cosurfactant. These aggregates can bring reactants together or to bring them apart and solubilize large amounts of sparingly water soluble compounds.

The kinetics and equilibrium of the formation of the ground state charge transfer complex between durene and chloranil was investigated in O/W microemulsions.

Electron transfer reactions between benzenediols and IrCl_6^{2-} and between IrCl_6^{3-} and 12-tungstocobaltate(III) were investigated over a wide range of microemulsion composition (from O/W to W/O). A three pseudo-phase model accounting for the observed rate constants was proposed.

Electron transfer reactions have been investigated also in cationic micellar systems and a model for the kinetics has been proposed.

Due to the importance of the solubilization of sparingly soluble organic compounds in micellar aggregates, the interaction of a series of differently substituted phenols with anionic micelles has been investigated. Group contribution to the binding constants has been evaluated for several substituents and their additivity

has been demonstrated.

The complexing and extracting properties of a functionalized surfactant family (4-alkylamidosalicylic acids) were investigated. The acid-base properties of the surfactant ligands, the partitioning and the kinetics of complex formation in the presence of non-ionic micelles were studied. The proper conditions for an efficient iron(III) complexation and extraction were determined.



Accession For	
NTIS	<input checked="" type="checkbox"/>
DTIC	<input type="checkbox"/>
Use for	<input type="checkbox"/>
A-1	

AD

COLLOIDAL ASSEMBLIES EFFECT ON CHEMICAL REACTIONS

Final Technical Report

by

Ezio PELIZZETTI

December 1988

United States Army

EUROPEAN RESEARCH OFFICE OF THE U.S. ARMY

London England

CONTRACT NUMBER DAJA 45-85-C-0023

Università di Torino, Italy

Approved for Public Release; distribution unlimited

Illustrations, Tables

Figure 1 - 24

Table 1 - 8

LIST OF PUBLICATIONS

- 1) V. Augugliaro, L. Palmisano, A. Sclafani, C. Minero, and E. Pelizzetti, "Photocatalytic Degradation of Phenol in Aqueous Titanium Dioxide Dispersions", *Toxicol. Environ. Chem.*, 1988, 16, 89.
- 2) M. Barbeni, M. Morello, E. Pramauro, E. Pelizzetti, M. Vincenti, E. Borgarello, and N. Serpone, "Sunlight Photodegradation of 2,4,5-Trichlorophenoxyacetic Acid and 2,4,5-Trichlorophenol on TiO_2 . Identification of Intermediates and Degradation Pathway", *Chemosphere*, 1987, 16, 1165.
- 3) E. Pelizzetti, M. Borgarello, C. Minero, E. Pramauro, E. Borgarello, and N. Serpone, "Photocatalytic Degradation of Polychlorinated Biphenyls in Aqueous Suspensions of Semiconductors Irradiated with Simulated Solar Light", *Chemosphere*, 1988, 17, 499.
- 4) R. Borello, C. Minero, E. Pramauro, E. Pelizzetti, N. Serpone, and H. Hidaka, "Photocatalytic Degradation of DDT Mediated in Aqueous Semiconductor Slurries by AML Simulated Sunlight", submitted.
- 5) E. Pelizzetti, V. Maurino, C. Minero, E. Pramauro, O. Zerbinati, and M. L. Tosato, "Photocatalytic Degradation of s-Triazine Pesticides", in preparation.
- 6) C. Minero, V. Maurino, L. Campanella, C. Morgia, and E. Pelizzetti, "Photodegradation of 2-Ethoxy- and 2-Butoxyethanol in the Presence of Semiconductor Particles or Organic Conducting Polymer", submitted.
- 7) E. Pelizzetti, V. Maurino, C. Minero, A. Sclafani, H. Hidaka, and N. Serpone, "Photocatalytic Degradation of Nonylphenol Ethoxylated Surfactants", submitted.
- 8) E. Pelizzetti, E. Pramauro, C. Maurino, N. Serpone, and E. Borgarello, "Photodegradation of Organic Pollutants in Aquatic Systems Catalyzed by Semiconductors", in "Photocatalysis and Environment", M. Schiavello ed., Kluwer Acad. Publ., Dordrecht, 1988, p. 469.
- 9) E. Pelizzetti, E. Pramauro, C. Minero, and N. Serpone, "Sunlight Photodegradation of Organic Pollutants Catalyzed by Semiconductor Materials", submitted.
- 10) M. Barbeni, C. Minero, E. Pelizzetti, E. Borgarello, and N. Serpone, "Chemical Degradation of Chlorophenols with Fenton's Reagent", *Chemosphere*, 1987, 16, 2225.

- 11) P.P. Infelta, R. Graglia, C. Minero, and E. Pelizzetti, "Ground State Charge Transfer Complexes in O/W Microemulsions", *Coll. Surfaces*, 1987, 28, 289.
- 12) C. Minero, E. Pelizzetti, and E. Pramauro, "Electron Transfer Reactions in Microemulsions: Oxidation of Benzenediols by Hexachloroiridate(IV)", *Langmuir*, 1988, 4, 101.
- 13) C. Minero, E. Pramauro, and E. Pelizzetti, "Reaction Kinetics as a Probe for the Structuring of Microemulsions", *Coll. Surfaces*, in press.
- 14) E. Pelizzetti, E. Pramauro, and C. Minero, "Kinetics and Reactivity in O/W Microemulsions", *Ann. Chim. (Rome)*, 1987, 77, 127.
- 15) C. Minero, E. Pramauro, and E. Pelizzetti, "Generalized Two-Pseudo-phase Model for Ionic Reaction Rates and Equilibria in Micellar Systems. Hexachloroiridate(IV)-Iron(II) Electron Transfer in Cationic Micelles", *J. Phys. Chem.*, 1988, 92, 4670.
- 16) E. Pramauro, C. Minero, G. Saini, R. Graglia, and E. Pelizzetti, "Partitioning of Phenols between Water and Anionic Micelles. Correlation with the Octanol-Water System", *Anal. Chim. Acta*, 1988, 212, 171.
- 17) E. Pramauro, C. Minero, and E. Pelizzetti, "Use of Amphiphilic Ligands in Chemical Separations", in "Use of Ordered Media in Chemical Separations", W.L. Hinze and D.W. Armstrong eds., ACS Symp. Ser., 1987, 342, 152.
- 18) F.P. Cavaasino, C. Sbriziolo, E. Pelizzetti, and E. Pramauro, "Kinetic and Equilibrium Studies of Complex Formation between Iron(III) and 4-Alkylamido-2-hydroxybenzoic Acids in Aqueous Nonionic Micellar Media", *J. Phys. Chem.*, in press.
- 19) E. Pramauro, E. Pelizzetti, C. Minero, E. Barni, P. Savarino, and G. Viscardi, "Properties and Applications of Amphiphilic and Hydrophobic Ligands", *Ann. Chim. (Rome)*, 1987, 77, 209.

Participating scientific personel

Edmondo PRAMAURO	Associate Professor
Claudio MINERO	Associate Researcher

CONTENT

I. Photodegradation of aromatic compounds by visible light	p. 1
- Phenol	
- 2,4,5-Trichlorophenoxyacetic acid	
- Other haloaromatic compounds	
- Triazine herbicides	
- Non-halogenated solvents	
- Non-ionic surfactants	
- Reviews. Comments	
II. Oxidative degradation of organic compounds	p. 12
III. Chemical reactions in microemulsions and micelles	p. 17
- Ground state complex formation in microemulsions	
- Redox reactions in microemulsions	
- Electron transfer reactions in micelles	
- Partitioning of substituted phenols in micelles	
IV. Characterization and properties of functionalized surfactants	p. 26
- Extraction and complexing properties of hydrophobic salicylic acids	
- Kinetics of complex formation in micellar media	
- Reviews. Comments	

I. PHOTODEGRADATION OF ORGANIC COMPOUNDS BY VISIBLE LIGHT

Semiconductor particles have been proved to be active catalysts in organic transformations induced by light. Since Chloroaromatic derivatives are compounds of relevant concern because some of them are bioaccumulative and persistent in the environment and also extremely toxic, their behavior under solar light has been investigated. In fact microbial degradation and naturally occurring hydrolysis require long periods; direct photodegradation requires high energy photons often leading to incomplete decomposition and, in some cases, to the formation of dangerous products.

Heterogeneous photo-assisted catalytic degradation by means of semiconductor particles has been applied to a variety of aromatic compounds.

The efficiency of these photocatalyzed reactions depends on many factors and mainly on the nature of the semiconductor. Figure 1 shows the results of light exposure of aerated aqueous solutions of 3,4 dichlorophenol in the presence of 2 g/l of various semiconductor suspension, at constant pH and temperature. The spectral distribution of irradiation (from a Solarbox lamp) in the experimental range 310-830 nm corresponded to AM1 solar illumination. The experiments concerning phenol and 3,4,5-trichlorophenoxyacetic acid degradation were carried out mainly with TiO_2 as photocatalyst.

I.1. Phenol

A typical experiment of phenol photocatalytic degradation is reported in Figure 2 where also the intermediate benzenediol (quinol and catechol, identified by LC) concentration is shown.

The salient features experimentally observed can be summarized as follows:

- the photodegradation is pH dependent and the highest photo reactivity is observed in the alkaline region;
- there is not degradation in absence of oxygen;
- the presence of massive amount of Cl^- negatively affects the degradation rate;
- the degradation rate is negatively affected by the initial phenol concentration;
- the reflectance spectrum of TiO_2 is not affected by the phenol adsorbed from a solution at pH 3, whilst it is affected when the phenol is adsorbed from a solution at pH 13, anatase being more photoactive than rutile;

- intermediate compounds are detected which are unstable and photodegraded.

An indication of the catalytic nature is obtained from the sunlight experiments, for which it was observed that the reaction proceeded for months without showing any decline. Moreover a rough calculation of the turnover number, molecules converted/(sites·h), gives a figure of about 200, showing that the surface sites are renewed 200 times in one hour. This calculation was made considering an initial rate of phenol photodegradation of $60 \text{ mg l}^{-1} \text{ h}^{-1}$, $5 \cdot 10^{14}$ surface OH^- sites/ cm^2 and that for the complete phenol oxidation 28 electrons are required.

It may be safely assumed that in the alkaline slurry the surface of TiO_2 is fully covered with water molecules and with OH^- groups; in a somewhat similar situation it has been demonstrated that OH^- groups and water molecules are roughly in a 1:1 ratio. The OH^- groups will likely exhibit a range of acid-base strength, according to the nature of the sites in which they are accommodated.

As far as the rate determining step of the process is concerned, it can be excluded any influence of mass transfer rate limitation to the solid-liquid interface. It would arise if the phenol and oxygen concentrations on the TiO_2 surface were practically zero. By calculating the ratio between the maximum mass transfer rate and the reaction rate, it comes out to be of the order of magnitude of 10^3 . This consideration indicates that the slow step in the phenol photodegradation process concerns the surface catalytic reaction because the liquid-solid mass transfer rate offers a negligible resistance.

We may therefore state that the photodegradation reaction occurs between the reactants both adsorbed on the TiO_2 surface. These adsorbed species as well as others present on the surface like OH^- will be involved in the reaction. Therefore the extent and the rate of the reaction is affected by the nature of the interaction between the reactants with the surface as well as by the electronic properties of the irradiated semiconductor.

The reflectance spectra of TiO_2 on whose surface phenol from a pH 13 solution, i.e. phenate ion, is adsorbed, clearly indicate that this species interacts with the surface forming a complex able to absorb visible radiation, while the phenate ions solution is photoactive in the UV region of the spectrum only.

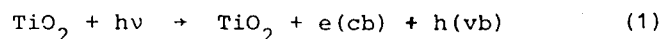
It is not straightforward to define how the phenate ions are bonded to a surface fully covered by water molecules and OH^- groups. We may only observe that the complex formed with the surface has an energy content higher than the ener

gy level of the phenate ion in solution and therefore it is prone to undergo a chemical transformation.

As for the oxygen, a variety of more or less stable species were detected according to the amount of hydroxylation, although there is a widespread agreement that the primary species in oxygen photoadsorption, in conditions similar to those used is O_2^- . Moreover it has been observed that oxygen photoadsorption is enhanced by the presence of hydroxyl groups while the presence of Cl^- groups, decreasing the OH^- content, decreases also the oxygen photoadsorption.

Having in mind the above considerations and also that, in absence of oxygen, no phenol photodegradation occurs, a tentative reaction scheme can be proposed.

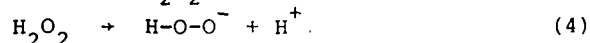
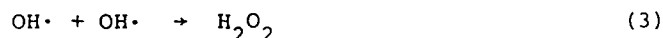
In a photocatalytic process the primary step is, of course, the photogeneration of pairs of electrons and holes which must be trapped to avoid recombination (charge separation):



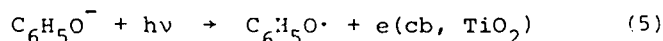
It is widely accepted that the hydroxyl groups are the likely traps for holes:



The possible destiny of $OH\cdot$ radicals can be described by the following reactions:

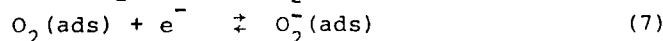
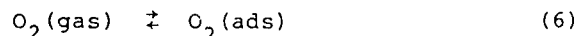


The peroxide ion is a well known oxidizing agent for organic substrates. In our case it must be also observed that, due to the fact that the surface phenate complex absorbs light at wavelength higher than that corresponding to the energy of the band gap of TiO_2 , the complex itself may act as sensitizer according the following reaction:

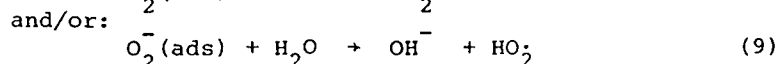
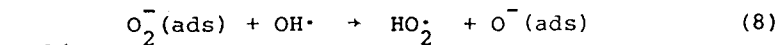


If this reaction takes place, then the phenate complex hastens the charge separation step and injects electrons to the conduction band of TiO_2 .

The traps for electrons are adsorbed oxygen species according to the following equations:

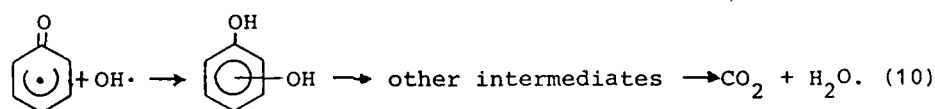


The superoxide species is unstable and reactive. It may evolve in several ways:

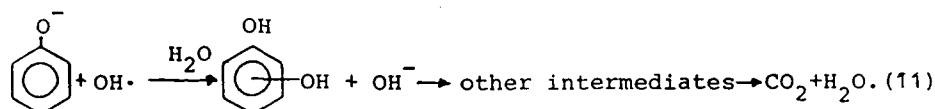


Thus as a consequence of the primary step of electrons and holes trapping, several species are produced, which will be involved in the reaction mechanism.

If the phenate ions act as sensitizer, thus forming radicals, these latter may likely evolve as follows:



In the phenate ion is still under an ionic form, the following scheme may be proposed:



The scheme proposed accounts for the main findings and indicates also the reasons why the photodegradation is lower in the acidic region. These reasons clearly are:

- the OH^- traps are much less in acidic medium than in the alkaline medium; therefore the charge separation step is less efficient;
- the reflectance spectra of TiO_2 , treated with phenol from acidic solution do not show appreciable change, indicating that the adsorption of phenol is very scarce;
- the chemisorption of O_2 in acidic medium is lowered with respect to the alkaline medium.

All these reasons affect in a negative way the course of the reaction in acidic medium. Finally it must be observed that adding Cl^- to the dispersions lowers the activity for the reasons already given. Of course this effect is much more evident in the acidic medium than in the alkaline medium where a very large amount of OH^- is present.

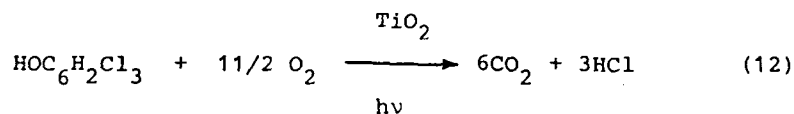
I.2. 2,4,5-Trichlorophenoxyacetic acid (2,4,5-7) and 2,4,5-Trichlorophenol (2,4,5-TCP)

As shown in Figure 1, chlorophenols can be photocatalytically degraded by semiconductor particles under visible light.

Because of its importance, the photocatalytic degradation

of 2,4,5-T has been investigated as well as that of 2,4,5-trichlorophenol which has been shown to be one of the major intermediate species.

Fig. 3a illustrates the complete degradation of 2,4,5-T and 2,4,5-TCP in aqueous suspensions of TiO_2 in the presence of air. Illumination ($\lambda > 340 \text{ nm}$) of $1 \times 10^{-4} \text{ M}$ of 2,4,5-T and 2,4,5-TCP in air and in the presence of suspended titanium dioxide results in the rapid disappearance of the chlorinated organic compounds with the concomitant formation of Cl^- (Fig. 3b). The amount of Cl^- (ca. $3 \times 10^{-4} \text{ M}$) and CO_2 formed confirms the complete mineralization of 2,4,5-T and 2,4,5-TCP. For example, 2×10^{-6} moles of 2,4,5-TCP gave 1.2×10^{-5} moles of CO_2 , according to the stoichiometric equation (12):



From the ratio between Cl^- formed and 2,4,5-T or 2,4,5-TCP degraded as a function of illumination time, it was observed that a difference exists between the degradation behaviour of the two chloro compounds; the ratio is 3 all along the reaction time for 2,4,5-TCP as expected from the stoichiometric decomposition (reaction 12). Such is not the case for the 2,4,5-T. In fact, only after 180 min of irradiation does the ratio between Cl^- formed and 2,4,5-T ($1 \times 10^{-4} \text{ M}$) consumed reach the value of 3, even though the total disappearance of 2,4,5-T from the solution occurs in less than 100 min (Figure 3).

According to these results, the degradation of 2,4,5-T, induced by irradiated TiO_2 dispersions, shows a very particular behaviour compared to the chlorophenols. In fact several intermediates were observed and identified by GC/MS after 20 min of irradiation under simulated AM1 conditions in aerated aqueous TiO_2 suspensions. The intermediate species were detected in a wide range of concentrations which showed to be crucial in proposing the several degradation pathways illustrated in Fig. 4. Of course, the identification of different intermediates is dependent on the stability of the intermediate itself as some of these species undergo further facile oxidation. As a consequence, observation and identification of trace quantities of an unstable intermediate product, as well as the high concentration of a very stable intermediate species contribute to the formulation of a plausible degradation mechanism. Trace amounts of different reaction products were analyzed by taking into account the contribution of the impurities present initial-

ly in 2,4,5-T as supplied by the vendor. Parallel analyses were carried out on the products from the treatment of the intermediate species with diazomethane in order to decrease their polarity and to better identify these products by mass spectrometric techniques.

2,4,5-TCP (III) and 2,4,5-trichlorophenyl formate (IV) are the two major and longer lived intermediate products of the photodegradation of 2,4,5-T. The OH^\bullet (and HO_2^\bullet) radicals generated through sequence (1)-(9) can subsequently undergo a series of reactions with the 2,4,5-T, leading to the products summarized in the scheme illustrated in Fig. 4. The details of the mechanism are not yet entirely clear; however, it seems plausible, by simple analogy with the photodegradation of 4-chlorophenol, that repeated hydroxyl attack on the aromatic ring will lead to chloride radicals and eventually also to some semiquinonoid type radicals. The Cl^\bullet radicals formed undergo subsequent reduction to Cl^- (reaction 13):



The semiquinone radicals formed can subsequently be oxidized (or can disproportionate), with the resulting benzoquinone undergoing further degradation via photocatalytic oxidation on TiO_2 as reported earlier. The photodegradation pathway reported in Fig. 4 is analogous to the mechanism proposed in the photochemical degradation of 2,4,5-T in the absence of TiO_2 , except that polymer formation was observed instead of complete mineralization to CO_2 and HCl when TiO_2 is present. It is worth noting that the simple process of dehalogenation appears not to be significant in the photocatalyzed degradation of 2,4,5-T reported here.

Finally, the activity of the TiO_2 Degussa P-25 powder was tested for the photodegradation of 2,4,5-T by performing several runs with the same TiO_2 powder: 1.5×10^{-4} M of 2,4,5-T was irradiated for 60 min leaving 1.1×10^{-5} M of non-decomposed substrate in solution. After this period, a fresh solution of 2,4,5-T was added and the photodegradation continued. This same cycle was repeated 11 times; the subsequent cycle was run for 120 min. At this point, the TiO_2 was washed with water, and then used again in the photodegradation process. From the results it is evident that the quantity of 2,4,5-T photodegraded with time is virtually constant and appears to have no consequence on the photo-activity of TiO_2 . This is taken to suggest that no adsorption of final products and no modification of the surface occur.

I.3. Other haloaromatic Compounds

Since it was shown that TiO_2 exhibits the highest efficiency in the photodegradation of halophenols, it was chosen to investigate the decomposition of the series of chloroaromatic compounds listed in Table 1.

From these data it is evident that the process can be applied to a wide variety of compounds, even when present at very low concentrations. The observed degradation half-life ($t_{1/2}$) seems to be only slightly affected by the increase in the halogen content as well as by the solubility of the compound; experiments have also demonstrated that photodegradation proceeds at a significant rate also under direct sunlight.

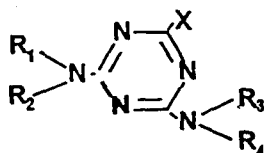
For compounds which are scarcely soluble in water, such as DDT, 3,3'-DCB or 2,7-DCDD, the experiments were performed after stirring the substrate dissolved in n-hexane with the semiconductor. Upon evaporation of the solvent the catalyst was suspended in aqueous media and irradiated.

In the case of DDT as well as dioxins and PCB's, the photocatalytic activity of some commercial powders of semiconductors was tested. As shown in Fig. 5, TiO_2 is the most active.

Interestingly for all these chlorinated compounds, which exhibit very long life in the environment, half-lives of 40-80 minutes are observed under photocatalytic conditions. However, for 2,7-dichlorodioxin only after 90 hours its concentration is reduced below 0.1 ppm from the initial concentration of 20 ppm (see Fig. 6) and even longer times are required for a complete mineralization.

I.4. Triazine herbicides

Triazines, compounds of general formula,



where $X = Cl, OCH_3, SCH_3$

and $R = H, \text{ alkyl group,}$

represent a very popular class of herbicides used to control broadleaf and grassy weeds in corn and also in sorghum, sugarcane, pineapple and other crops. Because of the persistence and the large and prolonged use, traces have been found in groundwater, sometimes exceeding the admitted threshold values.

The photocatalytic degradation of the compounds listed in Table 2 has been demonstrated. It is noteworthy that the process is still very efficient also at ppb levels (see Fig. 7). Interestingly some s-triazine derivatives are stable to photodegradation. Amino- and hydroxy substituted s-triazine have in fact been detected after long irradiation times. Work is in progress on this class of compounds.

1.5. NON-HALOGENATED SOLVENTS

Large volumes of solvent wastes are generated annually and their disposal represents a problem of relevant environmental concern. In many instances the organic solvents became mixed with water and the resultant aqueous waste stream can be treated in the framework of the several technologies improved in the last decade. Whereas photocatalytic mineralization of low molecular weight halogenated solvents on TiO_2 particles has been reported, little attention has been devoted to non-halogenated solvents.

The photodegradation of two low molecular weight non-halogenated solvents, namely 2-ethoxy- and 2-butoxyethanol, has then been investigated. In addition to the method which uses semiconductor particles suspended in the aqueous waste, another method with the use of organic conducting polymers has been tested.

Conductive polymers can be obtained by polymerization of monomers of suitable structure characterized by low redox potential and/or high electronic affinity. Doping of the obtained polymer with oxidizing or reducing agents yields a polymer with an ionic structure formed respectively by the cation of the polymer and the anion of the doping agent or viceversa. According to the nature of the polymer and the nature and concentration of the dopant, different values of cationic or anionic conductivity are observed for the doped polymer. Because of their polymeric nature, the preparation of a membrane based on these compounds is quite simple and easy.

The degradation in the presence of TiO_2 particles is depicted in Fig. 8, where in addition to the disappearance of the 2-butoxyethanol, CO_2 evolution as well as DOC and POC (Dissolved Organic Carbon and Particulate Organic Carbon, respectively) are monitored.

Interestingly Fig. 9 reports the degradation in the presence of organic conducting polymer, which has the advantage to be easily removed from the solution.

Work is in progress on this matter.

I.6 NON-IONIC SURFACTANTS

The photocatalytic degradation of non-ionic nonylphenol ethoxylate surfactants has been investigated using TiO_2 particulate as photocatalyst. Degradation processes have been monitored through liquid chromatography, CO_2 evolution and DOC and POC measurements. Fig. 10-12 show the degradation process and the complete conversion to CO_2 has been demonstrated.

The degradation routes involve, in the early part of the process a competitive attack of hydroxy radicals on the ethoxy chain and on the aromatic ring, which can be rationalized in the framework of a kinetic model that we are developing. A reaction scheme, illustrated in Fig. 12, can be proposed. Work is in progress also in this matter.

I.7. REVIEWS. COMMENTS

The photocatalytic processes leading to the degradation of organic compounds have been reviewed extensively by the present reporter (see ref. 8 and 9).

Comparison with the several thermal and non-thermal processes that can be used for treating organic wastes has been attempted. In fact, some of these are difficult to apply to water treatment and inasmuch as microbial degradation and naturally occurring hydrolysis require long period, methods involving the use of light can represent a valuable alternative. These possibilities are listed in Table 3.

The photocatalytic degradation method appears to be a "soft" technique requiring low-temperature and low-pressure conditions. In addition there are the following advantages:

- (i) complete destruction of the organic contaminants is generally observed in few hours
- (ii) the process seems to avoid the formation of photocyclized products
- (iii) the process requires a non-expensive catalyst with high turnover and that can be supported in proper reactors
- (iv) the process can be applied to contaminants present at concentrations very low, even in the ppb range.

In conclusion since the reaction conditions are mild and the reaction times relatively short, the future challenge will be from one side to have a better understanding of the fundamentals of photocatalytic processes and of the properties of the catalysts and from the other side to demonstrate the economic as well as the technical feasibility (proper and efficient photoreactors) of the heterogeneous photocatalytic treatment for the destruction of organic contaminants in aquatic systems.

II. OXIDATIVE DEGRADATION OF ORGANIC COMPOUNDS

The degradation of organic pollutants by chemical oxidation affords an alternative route to the biological and natural routes, especially at high concentration of the contaminants. As shown in the previous section I the heterogeneous photocatalytic degradation of Chloro aromatic compounds proceeds through mechanism(s) in which $\text{OH}\cdot$ radical species may intervene in the reactions at irradiated aqueous slurries of TiO_2 .

Similarly, Fenton's reagent ($\text{Fe}^{2+} + \text{H}_2\text{O}_2$) easily induces the degradation of chlorinated phenols if excess H_2O_2 is used and O_2 is present in the reaction mixture.

Fig. 43 depicts the decrease in concentration of differently mono substituted chlorophenols as a function of time. The results demonstrate that the 3-chlorophenol (3-CP) is rapidly degraded in the presence of a $\text{Fe}^{2+}/\text{H}_2\text{O}_2/\text{O}_2$ mixture; disappearance of the analogous 2-CP and 4-CP is slower under the same conditions. Concomitant with the degradation of these CP species, an equimolar amount of free chloride ions in solution was detected (Fig. 43). A parallel experiment performed on the same reaction batch, but using HPLC techniques to detect the fate of the chlorophenols or its intermediates showed complete degradation of the aromatic ring. This implicates the occurrence of an oxidative process and not merely a simple dehalogenation substitution reaction.

Analogous results were obtained for the dichlorophenols and trichlorophenols under identical conditions. In Table 2 are summarized the times necessary ($t/2$) to reduce the initial concentration of the chlorophenols in solution by a factor of two. It should be pointed out that this $t/2$ parameter is a practical operational parameter that includes any (if any) induction period to the start of the degradation reaction and must not be confused with the $t_{1/2}$ kinetic parameter for the reaction of disappearance. This $t_{1/2}$ procedure allows us to compare, in practical terms, the times required for the total degradation of these contaminants, even though the mechanism(s) may or may not be identical.

It is intriguing to note (cf. Fig. 43) that among the mono-chlorophenols, meta-chloro substitution induces a more rapid degradation than either of the ortho-chloro or para-chloro substitution. The differences in the rates of decomposition of these mono-chlorinated species is real. At higher $[\text{HClO}_4]$, the degradation is considerably inhibited as clearly noted in Table 4, which also summarizes $t/2$ values with changes in $[\text{HClO}_4]$. For the same HClO_4 concentration and for the same $\text{Fe}^{2+}/\text{H}_2\text{O}_2$ ratio, the 3,4-dichlorophenol (3,4-DCP) decomposes faster than any of the other compounds studied. In all cases, the stoichiometric quantity of free Cl^- was detected in solution at the completion of the reaction.

The formation of Cl^- is slower than the disappearance of the 3,4-DCP from the solution. Indeed, in a solution containing $3.0 \times 10^{-4}\text{M}$ of 3,4-DCP, $5.0 \times 10^{-5}\text{M}$ Fe^{2+} , $5.0 \times 10^{-3}\text{M}$ H_2O_2 and $5.0 \times 10^{-3}\text{M}$ of HClO_4 , the dichlorophenol disappears completely in < 25 min of reaction, while the expected stoichiometric amount of free Cl^- ($6.0 \times 10^{-4}\text{M}$) in solution for complete degradation of 3,4-DCP is obtained only after 250 min of reaction. This suggests that chloroaliphatic intermediate(s) may be formed after the opening of the benzene ring. This time lag between the disappearance of the phenol and the complete appearance of the product(s) (here, Cl^- ions) depends on the number of chloro substituents on the aromatic ring. For instance, for the mono-chloro derivatives, the disappearance of the chlorophenols and the appearance of stoichiometric amounts of chloride occur at nearly similar times (see Fig. 13). The results of Table 4 also indicate that a HClO_4 effect exists, and at higher concentrations of this acid the reaction is slower.

The disappearance of 3,4-DCP ($3.0 \times 10^{-4}\text{M}$) as a function of time, for three different concentrations of HClO_4 , is reported in Fig. 14: the other reagents were kept at $[\text{Fe}^{2+}] = 5.0 \times 10^{-5}\text{M}$, $[\text{H}_2\text{O}_2] = 5.0 \times 10^{-3}\text{M}$. Thus a tenfold increase of $[\text{HClO}_4]$, from $5.0 \times 10^{-3}\text{M}$ to $5.0 \times 10^{-2}\text{M}$, leads to an increase of $t/2$ from ~ 7 min to ~ 85 min. In the degradation of other chlorophenols, an increase of $[\text{HClO}_4]$ increases the induction period for the degradation process. A typical example is portrayed by the decomposition of 4-CP. Where $[\text{HClO}_4]$ is $1.5 \times 10^{-2}\text{M}$, no detectable degradation occurs for ~ 100 min. The $t/2$ is > 180 min (Table 4).

Another important parameter to consider was the effect of the Fe^{2+} concentration.

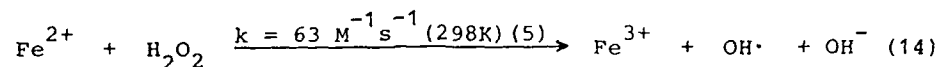
Increasing the $[\text{Fe}^{2+}]$ in solution for a fixed $[\text{H}_2\text{O}_2]$ at $5.0 \times 10^{-3}\text{M}$ increases the rate of decomposition. At concentration $> 2.0 \times 10^{-4}\text{M}$ in Fe^{2+} , the decomposition was too fast to follow with our techniques for reasonably reproducible results.

Finally the effect of Fe^{3+} on the degradation of 4-CP in a H_2O_2 /chlorophenol mixture was investigated. The reaction was carried out at 10^{-2}M in HClO_4 . Addition of Fe^{3+} (instead of Fe^{2+}) is inconsequential in the degradative process. However, an equivalent concentration of Fe^{2+} brings $t/2$ to ~ 50 min.

Equimolar amounts of Fe^{3+} and Fe^{2+} in the same reaction mixture increase the reaction rate ($t/2 \sim 20$ min). No doubt, Fe^{3+} is an important species in the complex degradative process.

The results herein reported may be interpreted on the basis of the following considerations. The interaction of iron(II) ions with hydrogen peroxide yields OH^\bullet radicals and iron(III)

(equation 14). The $\text{OH}\cdot$ formed, can easily



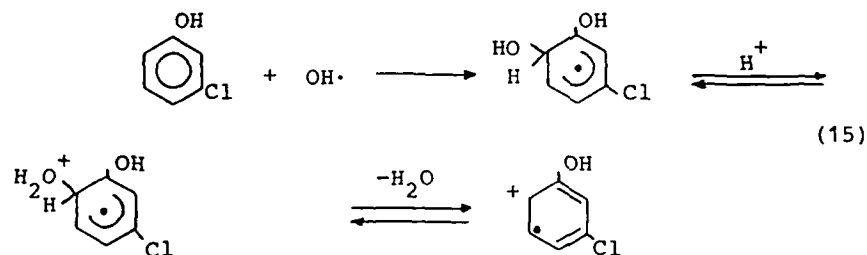
interact with an aromatic compound inasmuch as $\text{OH}\cdot$ radicals are good electrophiles.

In the presence of oxygen, oxidation of the intermediate species ($\text{HOCl}\dot{\text{C}}_6\text{H}_3\text{H}(\text{OH})$) is preferred even if dimerization is still possible.

By analogy with earlier work on hydroxylations of aromatics, the degradative oxidation of chlorophenols probably proceeds via a hydroxylated species following which ring opening occurs to yield aldehydes and ultimately degradation ensues to CO_2 and Cl^- .

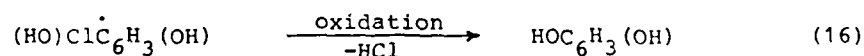
Various factors may contribute to the above experimental observations.

It can be tentatively suggested as a first step the formation of a radical cation by acid-catalyzed dehydration of the radical formed between the interaction of $\text{OH}\cdot$ with the chlorophenols (reaction 15). Evidences of the formation of radical-cations in acid media have been reported for methoxylated benzoic



acids. The different stabilities of the radical-cations formed for other chlorophenols may be an important factor responsible for the induction period observed in the degradation of chlorophenolic compounds at higher acidity. In fact, chlorine substituents in ortho and para positions can stabilize the positive charge of the radical-cation of eq. 15 better than meta-chlorine.

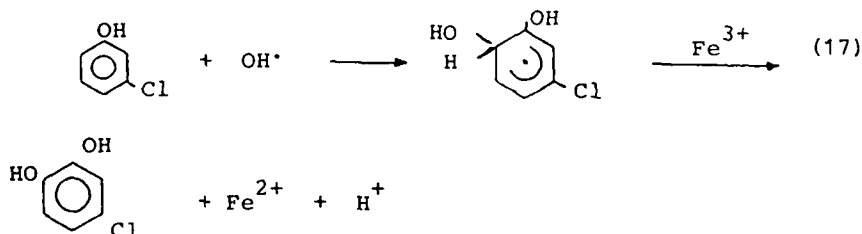
An alternative route of degradation is shown in eq. 16:



The formation of resorcinol as an intermediate product in the degradation reaction of 3-CP has been detected by HPLC technique.

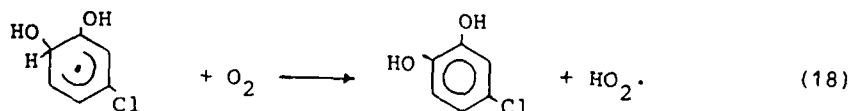
The increase in the oxidation rate of the decomposition of these chlorinated aromatic substrates when the amount of Fe^{2+} is increased from $3.0 \times 10^{-5}\text{M}$ to $2.0 \times 10^{-4}\text{M}$ is the result of an increase in the concentration of $\text{OH}\cdot$ produced according to reaction 14. Under our experimental conditions, it was not possible to investigate the process at higher $[\text{Fe}^{2+}]$ as the reaction was too rapid, even at higher $[\text{HClO}_4]$.

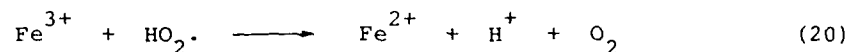
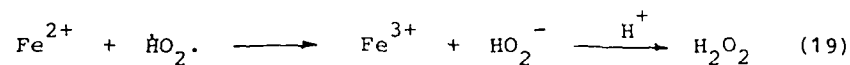
Iron(III) alone with H_2O_2 has very little effect, if any, on the degradation reaction (no $\text{OH}\cdot$ radicals can be formed). However, inasmuch as $\text{HO}_2\cdot$ radicals form from $\text{Fe}^{3+}/\text{H}_2\text{O}_2$ mixtures, these are inconsequential in the first step of the decomposition. Equivalent amounts of Fe^{2+} and Fe^{3+} increase the rate of oxidation more than the presence of Fe^{2+} alone. Furthermore, in a typical experiment (cf. Table 4), the amount of Fe^{2+} is catalytic compared to H_2O_2 and chlorophenol concentrations. Since reaction 14 is stoichiometric and almost complete degradations of the chlorophenols are obtained, reduction of Fe^{3+} to Fe^{2+} must occur. These considerations suggest the possible occurrence of reaction 17. That $\text{Fe}^{2+}/\text{Fe}^{3+}$ mixtures enhance the



degradation of the chlorophenols, while the presence of a large concentration of HClO_4 inhibits the reaction, is indicative of the competitiveness of reactions 15, 16 and 17.

Oxygen also has an effect on the hydroxylation reactions since it can act as a radical scavenger as noted in reaction 18. Following this, the $\text{HO}_2\cdot$ species can successively react with either Fe^{2+} or Fe^{3+} (reaction 19,20) to regenerate H_2O_2 and Fe^{2+} .





Further reaction of these hydroxylated aromatic species with the oxidizing agents in solution leads to the degradation products.

The disappearance of chlorophenols and appearance of free chloride in solution (Fig. 13) follow neither first nor second order kinetics, which appear to be quite complex. Further studies will address the nature of the various species in the hope of clarifying the pathway(s) of the degradation process.

Comments

These studies have shown that the utilization of Fenton's reagent affords an attractive possibility of decomposing chlorinated aromatic contaminants. Other studies, in program are directed at the potential degradation of pollutants and may contribute to the resolution of environmental problems such as the control and disposal of wastes.

III. CHEMICAL REACTIONS IN MICROEMULSIONS AND MICELLES

Microemulsions are transparent dispersions of an oil in water (O/W) or water in oil (W/O) in the presence of a surfactant and a cosurfactant.

These dispersions form spontaneously upon mixing and contain spherical droplets, having usually diameters of 10-60 nm. The O/W microemulsions have similarities to normal micelles in water, and can be described as a stable collection of "oil" microdroplets in an aqueous continuous phase, while W/O microemulsions should be similar to the reverse micelles in apolar solvents.

The submicroscopic aggregates can bring reactants together or keep them apart, and can also exert a medium effect. As reaction media however the microemulsions can incorporate relatively large amount of solute and the volume of the disperse phase can generally be varied over a fairly wide range.

Whereas reactions in micelles have been studied extensively, processes in microemulsions (particularly electron transfers) have been scarcely examined.

Two model reactions (see below) have been investigated in order to obtain informations on the properties of microemulsions as reaction media.

III.1. Ground State Charge Transfer Complexes in O/W Microemulsions

Solute migration in microheterogeneous media still raises a number of questions as to its rates and mechanism.

In aqueous micellar solution, a number of investigations have led to a reasonable understanding of the solubilization of solutes as well as some of the mechanisms of their migration. For example, a dynamic exchange of CH_2I_2 takes place between bulk and sodium dodecylsulphate (10^{-1} M) micelles at a rate of the order of 10^7 s^{-1} . It is clear however that the rate of such processes is highly dependent upon the hydrophobic/hydrophilic character of the solute, as well as the nature of the microheterogeneous aggregates.

In order to clarify this point the formation of the ground state charge transfer complex between durene and chloranil was investigated in CH_2Cl_2 and in oil-in-water (O/W) microemulsions. The CH_2Cl_2 or CH_2Cl_2 /hexadecane microemulsion systems are stabilized by a cationic (hexadecyltrimethylammonium bromide) surfactant and 1-butanol as cosurfactant.

Since the equilibrium constant for the formation of charge transfer complex is 0.66 M^{-1} in CH_2Cl_2 and 8.4 M^{-1} in μE ,

it is evident that the compartmentalization introduced by the microemulsion structure favors drastically the CT complex formation.

If one writes the law of mass action with respect to the non-aqueous volume, one would expect to have

$$\frac{|DA|_o}{|D|_o |A|_o} = K_H \quad (21)$$

where concentrations are measured with respect to the oil phase. This may be transformed to use average concentration (with respect to the total volume). One obtains

$$\frac{|DA|}{|D| |A|} = K_H \frac{V_t}{V_o} = K_M \quad (22)$$

where V_t is the total solution volume and V_o is the "oil phase" volume. From the measured K_H and K_M one obtains that V_t/V_o should be 12.6.

Under the assumption that there is no change in the density of water in the microemulsion systems, the ratios V_t/V_o for the two microemulsions can be evaluated to be ca. 3, which does not account for the experimental ratio K_M/K_H . For the O/W systems considered here, the structure of the droplets may be described as a stable collection of "oil" microdroplets in an aqueous continuous phase. Each droplet consists of a "bulk" oil drop surrounded by a thick interphase consisting mainly of alcohol molecules and cationic surfactant. Then, if the ratio V_t/V_o is calculated as $\Sigma(w_i/d_i) / \Sigma(w_o/d_o)$ (where d is the density, the subscript o refers to CH_2Cl_2 and hexadecane and i to all the components) values ranging from 7 to 10 can be estimated (depending on the microemulsion and on the assumptions concerning the density of the non-oil material).

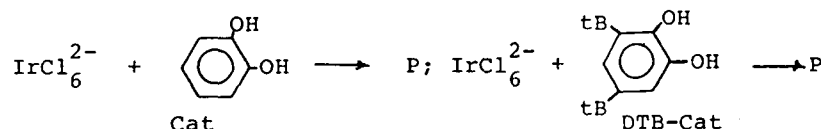
Thus, if the charge transfer complex is confined in CH_2Cl_2 or CH_2Cl_2 /hexadecane component, the change in the equilibrium constant from homogeneous to microemulsion medium should mainly be due to the decrease of the available volume for the solutes (A and D) in the microemulsion system. In this last hypothesis, the apparent lack of effect of the compartmentalization should be related to the solute (or complex) dynamic exchange between microemulsion droplets.

Using stopped-flow experiments, attempt was performed to measure the rate at which equilibrium is attained when mixing two identical microemulsions, one containing D and the other containing A, or one containing the charge transfer com

plex and the other only the microemulsion. Under all conditions, the expected equilibria were reached faster than the 1 millisecond time response of our equipment. Whatever the mechanisms involved we can say that equilibrium is obtained at a rate faster than $1 \times 10^3 \text{ s}^{-1}$.

III.2. Electron Transfer Reactions in μE

Degradation reactions often go through initial redox steps. As an example of electron transfer reaction involving organic substrates and oxidizing metal complexes in μE systems the following reactions have been selected:



- Pseudoternary phase diagram

The single-phase limits were experimentally determined (Fig. 15). By comparison with other phase diagrams reported for the same Butanol/SDS ratio, and from conductivity measurements (Fig. 16), it can be assumed that the microstructure changes from swollen micelles, through a bicontinuous phase, to reverse micelles. Whereas the lower phase limits can be explained by various current theories, the upper limit can be rationalized in terms of a failure of the bulk aqueous phase. The kinetic measurements were performed along the dilution lines, in which the Butanol/SDS/Toluene ratio was kept constant (see Fig. 15).

- Kinetic measurements

The variation of k_{exp} measured by stopped-flow as a function of the microemulsion composition is depicted in Fig. 17. For both investigated catechols, the following behavior has to be noted: - at higher water fractions inhibition is observed (which is more pronounced for DTB-Cat); - at lower water content there is an increase in reaction rates inversely dependent on the oil content.

- Three pseudophases model

A simple microemulsion model, consisting of three distinct pseudophases, without any assumptions about the microstructure, is proposed.

The following kinetic equation holds:

$$k_{\text{exp}}^{\mu\text{E}} = \chi_w \delta_w k_w \frac{\bar{C}_A(w) \bar{C}_B(w)}{C_A(\text{Tot}) C_B(\text{Tot})} + \chi_I \delta_I k_I \frac{\bar{C}_A(I) \bar{C}_B(I)}{C_A(\text{Tot}) C_B(\text{Tot})} + \chi_o \delta_o k_o \frac{\bar{C}_A(o) \bar{C}_B(o)}{C_A(\text{Tot}) C_B(\text{Tot})} \quad (23)$$

where: k is the second order rate constant in the micro-emulsion; δ 's are the densities of the microemulsion and of pseudophases; k 's are the specific rates constants in each phase; C 's are the local concentrations of the reagents expressed in moles/mass; x 's are the pseudophases molar fractions.

The partition coefficients for each reagent R ($A = \text{IrCl}_6^{2-}$, $B =$ catechols), are defined as follows: P_{WI}^A , P_{WI}^B , P_{WO}^A , P_{WO}^B , where:

$$P_{WF}^R = \exp\left(\frac{M_W^{OR} - M_F^{OR}}{RT}\right) = \frac{\chi_F^R \delta_F^R}{\chi_W^R \delta_W^R}$$

By substituting into equation (23):

$$k_{\text{Exp}} = \frac{\frac{k'_W}{\chi_W} + \frac{k'_I}{\chi_I} P_{WI}^A P_{WI}^B R_I^2 + \frac{k'_O}{\chi_O} P_{WO}^A P_{WO}^B R_O^2}{(1 + P_{WI}^A R_I + P_{WO}^A R_O)(1 + P_{WI}^B R_I + P_{WO}^B R_O)} \quad (24)$$

where $k' = k \cdot \delta$, $P_{WF}^R = P_{WF}^R \cdot \delta_W^R / \delta_F^R$, $R_I = (\sum_i n_i)_I / (\sum_i n_i)_W$, $R_O = (\sum_i n_i)_O / (\sum_i n_i)_W$.

In order to solve the equation (24), it is necessary to calculate the terms R_I and R_O .

Some assumptions about the composition of each pseudophase must be made:

$$(\sum_i n_i)_W = n_{W(W)} + n_{\text{But}(W)} \quad (25)$$

$$(\sum_i n_i)_I = n_{W(I)} + n_{\text{But}(I)} + n_{\text{SDS}(I)} + n_{\text{Tol}(I)} \quad (25)$$

$$(\sum_i n_i)_O = n_{\text{But}(O)} + n_{\text{Tol}(O)}$$

Thermodynamics imposes that the components present in each pseudophase must be in equilibrium. The eq. (24) and the appropriate mass balances can be solved in terms of mass transfer constants and activity coefficients. Since the system is far from ideality, another approach which takes in account the mutual solubility limits between the components, can be also proposed.

The moles of the components in each pseudophase can be related through proportionality constants α . It is assumed, in other words, that each pseudophase is always saturated with respect to the components present in defect. α 's coefficients are in fact solvation numbers.

$$\begin{aligned} n_{\text{But}(W)} &= \alpha_1 n_{W(W)} ; n_{W(I)} = \alpha_2 n_{\text{SDS}(I)} + \alpha_3 n_{\text{BUT}(I)} \\ n_{\text{But}(O)} &= \alpha_4 n_{\text{Tol}(W)} ; n_{\text{Tol}(I)} = \alpha_5 n_{\text{SDS}(I)} \end{aligned} \quad (26)$$

where α_1 represents the solubility of n-Butanol in water (0.017); α_2 is the hydration number for SDS in the interphase; α_3 is the solubility of water in n-Butanol (ca.1); α_4 is the solubility of n-Butanol in Toluene (); α_5 represents the average number of Toluene molecules per surfactant. It is obvious from these assumptions that the present model is not valid at the corners of the phase diagram.

- Analysis of the experimental data

The multiparametric kinetic equation was solved by computer simulation using eq. (24), (25), (26) with the following assumptions:

a) partition of microemulsion components. Since the solubilities of Butanol in water and Toluene are very low, $\alpha_1 = \alpha_4 = 0$. α_2 and α_3 are fitted by assuming that the upper demixing line is due to the failure of the aqueous pseudo-phase. The best fitting curves gave the following values: $\alpha_1 = \alpha_4 = 0$, $\alpha_2 = 3-3.5$, $\alpha_3 = 1$, and $\alpha_5 = 1$. The hydration number for SDS (α_2) is in agreement with the literature data.

b) partition of reagents: P_{WF}^{IR} is assumed to be constant. The estimated P_{WF}^{IR} values for catechols have to be consistent with the partition data obtained both from kinetic and HPLC measurements for SDS, whereas $P_{WF}^{IrCl_6^{2-}}$ must be very low.

c) kinetic parameters. k_W was measured as a function of dissolved Butanol. We used in the fitting the k_W value obtained in Butanol-saturated solution. k_I is a fitting parameter ($k_{But} \leq k_I \leq k_W$. k_{But} is the specific rate in the water-saturated Butanol solution). In eq. (24) the term depending on k_0 was neglected.

On the basis of the above mentioned assumptions, the fitting parameters to be evaluated are: P_{WI}^B , P_{WI}^B , P_{WI}^A , k_I .

The obtained fitting curves are shown in Fig. 17.

They were calculated using the following values:

	$k_W(\text{exp})$	k_I	$P_{WI}^{IrCl_6^{2-}}$	P_{WI}^{Cat}	P_{WO}^{Cat}
Cat	$3.9 \cdot 10^3$	$7.5 \cdot 10^3$	0.2	25	35
DTB-Cat	$7.0 \cdot 10^4$	$3.2 \cdot 10^4$	0.2	$5.0 \cdot 10^4$	$5.0 \cdot 10^5$

where $P_{WF}^{IR} = 55.5(K_B^R + \bar{v}_r)$; \bar{v}_r is the molar volume of the interphase; K_B^R is the usual binding constant (M^{-1}).

The previous hypotheses have been further tested by investigating an electron transfer reaction between two polycharged anions in the same microemulsion medium (i.e. SDS/l-butanol/toluene/water-0.09 M NaCl - 0.01 M HCl). The test reaction was the electron transfer reaction between hexachloroiridate(III) and 12-tungstocobaltate(III). The charge of the surfactant and the charge and the low hydrophobicity of the reagents ensure that the reaction would take place in the water pseudophase, and thus that the reaction rates would be sensitive to the 'effective volume' of the aqueous region. The reactants play the role of local probes in microemulsion medium and thus it will be possible to infer also some remarks about the structure of the microemulsion in the surfactant- or in the oil-rich region.

The experimental rate constants as function of the microemulsion composition are reported in Fig. 18, where the dilution lines correspond to a fixed ratio between SDS/l-butanol/toluene. It can be noted that at low water content there is an increase in the reaction rates, with respect to the aqueous solution, which is dependent on the oil content. For dilution lines with high oil content the rate diverges asymptotically when the upper demixing line is approached. In absence of oil (line 0) the increase is quite low and it is comparable with the increment due to the ionic strength. The rate constants measured along dilution lines 1 and 2 have a behavior intermediate between line 0 and lines 3,4,5.

The equation previously proposed is not able to predict the observed kinetic behavior for all microemulsion compositions if α values are taken constants. The fitting curves are shown in Fig. 18 as dashed lines. The value of p_2 for IrCl_6^{3-} of 0.15 was taken comparable with that of IrCl_6^{3-} evaluated previously, while the partition coefficient of the 12-tungstocobaltate(III) is found slightly less, 0.02. This value is consistent with the anion charge and its very low hydrophobicity. The simultaneous fitting of the upper demixing line and of the kinetic data on dilution lines 3,4,5 require that the degree of dissociation of the surfactant will be quite high, i.e. $\alpha = 0.55$, but still reasonable if almost all the alcohol lies in the surfactant palisade of the interface. In fact the value of α for micelles increases when alcohol is added.

COMMENTS

The proposed three pseudophase model is able to predict quantitatively the rate of reaction in microemulsion, in regions of the phase diagram where the solution is structured. The partition coefficients for reagents, the hydration number of the surfactant, and also the mean degree of dissociation agree quite well with reported or estimated values obtained using other techniques.

The comparison between kinetic data for a proper reaction and the prediction of the model, makes a clear distinction between microemulsion compositions which lead to a structured and a non-structured systems and allows to obtain some information on the hydration of the surfactant and of the cosurfactant without assuming any microscopical geometrical configuration of the solution.

The microemulsion systems appear suitable media for carrying out redox reactions involving highly hydrophobic compounds and hydrophilic metal complexes.

The kinetics and mechanism of reactions in O/W microemulsions have been extensively reviewed (ref. 14).

III.3 Electron Transfer Reactions in Micelles

A general phenomenological approach based on

- (i) the two pseudophase approximation
- (ii) a proper definition of the transfer constants between the pseudophases in term of molar fractions
- (iii) an explicit hypothesis that relates the number of bound molecules or ions to the surfactant concentration
- (iv) a semiempirical calculation of the activity coefficients of bound charged species at the micellar surface

permits the prediction of the reactivity as a function of micelle and added salt concentrations.

Kinetic experiments were designed to test the model; the investigated system was the electron transfer reaction between hexachloroiridate(IV)-Iron(II) in the presence of hexadecyltrimethylammonium chloride or sulfate with added sodium chloride or sulfate.

The fit with the model is shown in Fig. 19.

The dissociation degree of the micelle is found comparable with literature values.

III.4 Interactions of Solutes with Micelles

The partition equilibria of a series of thirty substituted phenols bearing different chemical groups between aqueous solutions and sodium dodecylsulfate micelles has been investigated by using micellar high-performance liquid chromatography and by studying the variation of the acidity constant.

The contribution of each substituent to the free energy of transfer from water to micelles has been estimated. Values are listed in Table 5 and 6.

The group contribution approach is shown to be valid for polysubstituted compounds under well defined conditions, as shown in Fig. 20.

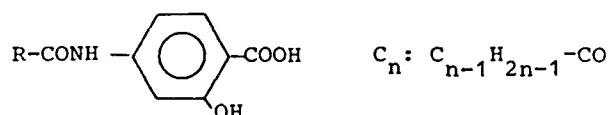
A comparison with partition coefficients obtained in classical two-phase system (1-octanol/water) is discussed.

IV. CHARACTERIZATION AND PROPERTIES OF FUNCTIONALIZED SURFACTANTS

Functionalized surfactants are amphiphilic molecules in which the polar head group can exhibit a chemical reactivities, such as complexing capability or electron transfer properties.

The complexing behavior could be used in chemical separations and in catalytic processes in organized assemblies.

As model system, the properties of a series of compounds containing the same chelating moiety, namely 4-aminosalicylic acid, with different alkyl chains, was investigated. The structure of the ligands (PAS-C_n) is the following:



Since aggregation occurs for these compounds only at high pH values, a study of complexing properties of aggregates in the presence of usual transition metal ions cannot be performed. At lower pH, however, the PAS-C_n molecules can be readily solubilized in the presence of nonionic surfactants (e.g. Brij 35: polyoxyethylene(23)dodecanol) and the obtained mixed micelles exhibit complexing capability in acidic media.

- Binding Constants of Ligands with Nonionic Micelles

The acid-base properties of the amphiphilic ligands change in the presence of micellar aggregates due to the well known partition equilibrium of both the acid and anionic form. A continuous increase in the apparent pK_a was observed with increasing concentration of micellized surfactant.

According to the simple pseudophase model of Berezin, the binding constants between the ligands and the micelles have been calculated using the following equation:

$$K_{a(\text{app})}^{-1} = K_{a(w)}^{-1} + K_{\text{HA}} \cdot K_{a(w)}^{-1} \cdot C_D \quad (27)$$

where K_{a(app)} is the dissociation constant of carboxylate group in the presence of Brij 35, K_{a(w)} is the same constant in water, K_{HA} is the binding constant of the undissociated PAS-C_n to the micelles and C_D is the concentration of micellized surfactant (C_D = C_{tot} - CMC).

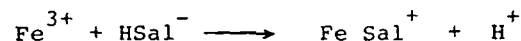
The critical micellar concentration for Brij 35, measured with the surface tension method is 6x10⁻⁵ M, in the experimental conditions.

For the investigated PAS-C_n ligands, the binding constant

for the undissociated form clearly increases with n , from 170 M^{-1} for C_2 and 500 M^{-1} for C_4 up to ca. 1500 M^{-1} for C_7 , whereas for the anionic form it becomes significant only for C_7 (110 M^{-1}). The obtained data is in good agreement with the values estimated from $\text{pK}_{a(\text{app})}$ shift, at low surfactant concentration, and allow us to define a minimum chain length for the ligand in order to have a strong binding to the micelles, both in acidic or anionic form.

- Complex Formation Constant in the Presence of Micelles
The kinetics and the complex formation equilibria in the presence of nonionic micelles have been also investigated, at constant acidity. The stoichiometry was assessed by using Job's method and the apparent stability constants were evaluated according to Frank and Ostwalt procedure, as previously reported for the system iron/salicylate in homogeneous aqueous solution.

For the equilibrium reaction:



where HSal^- indicates the dissociated chelating moiety of the ligand, the observed changes in the apparent formation constants (K_C) can be directly related with the variation of the apparent pK_a , previously discussed. In the conditions reported in the experimental section, the K_C values lie in the range $(2.5-4.0) \times 10^3$.

The experiments performed clearly showed that, whereas the complexation of iron(III) is not very much dependent on the ligand hydrophobicity, the association of the charged 1:1 chelates to the micelles and then the efficiency of the concentration process, markedly increases.

- Extraction of Iron(III) from Micellar Solutions

The surfactant system Triton X 100 / BL 4.2 was chosen because its suitable cloud temperature range and the good solubilizing capability towards the ligands.

The analyte content, after extraction, was determined both in the micellar and in the aqueous rich phase by VIS-spectrophotometry. Calibration curves were made with micellar phases containing the dissolved ligands, in the absence of iron (III). To these solutions, separated by centrifugation, were added known amounts of analyte and the absorbances were recorded.

The standard addition method was also applied to the extracted micellar layers containing iron(III). The results obtained with both procedures were in good agreement, as well as which obtained from DC-plasma spectrometry after analysis

of the aqueous dilute phases.

The extraction efficiency was then calculated from at least four independent measurements; the influence of the experimental parameters was also investigated.

Fig. 21 shows the effect of the ligand hydrophobicity on the analyte recovery, measured at pH 3.5, in the presence of Triton X-100 (1% w/v) and BL 4,2 (1% w/v); added NaNO_3 : 5% w/v; iron(III): $1 \times 10^{-4} \text{ M}$ and PAS-C: $2 \times 10^{-3} \text{ M}$.

As it can be seen, quantitative recovery of iron(III) has been obtained in the reported conditions using the more hydrophobic compounds (PAS-C₁₀ or higher analogues). However, the lower solubility of these long chain molecules can limit the ligand concentration available in the system, keeping the volume of extraction micellar phase constant.

The extraction performances under different experimental conditions (i.e. varying the pH, the composition of surfactant mixtures, the amount of chelating compound) were also investigated for our test system. The results are shown in Table 7.

- Kinetics of Complex Formation in Micellar Media

The kinetics for complexation reactions of Iron(III) with the PAS-C_n ligands (n= 2 and 4) was studied by stopped-flow technique in aqueous acidic solutions containing varying amounts of the non ionic micelle forming surfactant Brij-35.

The kinetic findings indicate that the complexation reactions occur in the aqueous intermicellar phase and that the reactions of the FeOH^{2+} ion with both the neutral and monoanionic forms of the ligands contribute significantly to the overall complex formation rate, a dissociative ion-pair mechanism being operative. The reaction scheme is depicted in Fig. 22.

The resulting kinetic expression is

$$\frac{1}{k_f} = \frac{K_{s,w} + [\text{H}^+]}{k_{f,w} K_{s,w}} + \frac{(K_{s,w} K_L' + K_L [\text{H}^+]) C}{k_{f,w} K_{s,w}}$$

and the experimental data plotted accordingly are reported in Fig. 23 and 24.

The binding constants of the iron(III) monocomplexes and the neutral ligands to the nonionic micelles were estimated from the equilibrium and kinetic data, respectively, and collected in Table 8.

- Comments

The results obtained with the reported amphiphilic ligands in the extraction process showed that the separation of charged species is possible, provided a suitable ligand hydrophobicity. Further developments of these multiphase extraction systems will require an accurate investigation of the equilibria and kinetic processes occurring at the interfaces, as well as the study of the micellar structure and properties of the host aggregates.

Other functionalized surfactants having various complexing groups and modular lipophilic chains, together with different nonionic solubilizing surfactants, are presently under investigation.

The general features have been reported in an exhaustive review (ref. 19).

Table 1.- Half-lives for the Total Photodegradation of Contaminants Assisted by TiO_2 on Exposure to Simulated Sunlight^a.

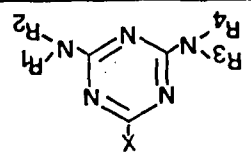
COMPOUND	ABBREV.	CONCENTRATION (ppm)	pH	$t_{1/2}$ (min)
4-chlorophenol ^b	4-CP	6	3.0	14
3,4-dichlorophenol	3,4-DCP	18	3.0	45
2,4,5-trichlorophenol	2,4,5-TCP	20	3.0	55
Pentachlorophenol ^b	PCP	12	3.0	20
Sodium pentachlorophenate	NaPCP	12	10.5	15
Chlorobenzene	CB	45	2.5	90
1,2,4-trichlorobenzene	1,2,4-TCB	10	3.0	24
2,4,5-trichlorophenoxyacetic acid	2,4,5-T	32	3.0	40
4,4'-dichlorodiphenyltrichloroethane ^c	4,4'-DDT	1	3.0	46
3,3'-dichlorobiphenyl ^c	3,3'-DCB	1	3.0	10
2,7-dichlorodibenzo-p-dioxin ^c	2,7-DCDD	0.2	3.0	46

^a: Concentration of catalyst, 2.0 g/l; aerated aqueous solutions; wavelength >330 nm.

^b: Wavelength >310 nm.

^c: Adsorbed on TiO_2

TABLE 2

Formula generale	Nome Chimico	Nome Comune	X	R ₁	R ₂	R ₃	R ₄
	2-cloro-4-etilammino-6-isopropilammino-1,3,5-s-triazina	ATRAZINA	Cl	H	C ₂ H ₅	H	CH(CH ₃) ₂
	2,4-disopropilammino-6-metossi-1,3,5-s-triazina	PROMETONE	OCH ₃	H	CH(CH ₃) ₂	H	CH(CH ₃) ₂
	2,4-diisopropilammino-6-metiltio-1,3,5-s-triazina	PROMETRINE	SCH ₃	H	CH(CH ₃) ₂	H	CH(CH ₃) ₂
	2-cloro-4-dietilammino-6-etilammino-1,3,5-s-triazina	TRIEATAZINA	Cl	H	C ₂ H ₅	C ₂ H ₅	C ₂ H ₅

- Erbicidi s-triazinici studiati.

Direct Photolysis	Ref. 4	Notes High energy photons; chloroorganic compounds; residues; cyclization compounds.
Indirect Photolysis	5, 122	Solar light; Sensitized required (stability problems); non complete degradation.
Ozone/hv	119	Ozone generator; Ozone storage difficulty; UV lamp required; effective degradation obtained.
H ₂ O ₂ /hv	120	Chemical reactant; UV lamp H ₂ O ₂ required; easy to mix; H ₂ O ₂ can not be stored; effective degradation obtained.
Photocatalysis	this work	Heterogeneous system; Solar radiation or UV lamp required; complete mineralization; stable catalyst; no chemical reactant required; applicable to waste water and to drinking water.

TABLE 3
Comparison of degradation methods involving light.

TABLE 4 - Half-lives ($t/2$; see text) of Decomposition
of Various Chlorinated Phenols: $[\text{Fe}^{2+}] =$
 $5.0 \times 10^{-5} \text{ M}$, $[\text{H}_2\text{O}_2] = 5.0 \times 10^{-3} \text{ M}$,
 $[\text{chlorophenols}] = 3.0 \times 10^{-4} \text{ M}$.

Compound	$t/2$ at $5.0 \times 10^{-3} \text{ M}$	$t/2$ at $1.5 \times 10^{-2} \text{ M}$
	HClO_4 (min)	HClO_4 (min)
3-chlorophenol	6.5	34
2-chlorophenol	14.5	125
4-chlorophenol	12.5	> 180
3,4-dichlorophenol	6.3	16
2,4,5-trichlorophenol	12	36

TABLE 5

Binding of substituted phenols to SDS micelles and standard energies of transfer per molecule and per group

No.	Compound	$K_H (M^{-1})$	$\Delta\mu_c^0 (kJ mol^{-1})$		Log $P_{o/w}^*$
			Molecule	Group	
1	Phenol	10 ^h	-15.66	-	1.46
2	4-Methoxy	15 ⁱ	-16.65	-0.99	1.34
3	4-Ethoxy-	27.5 ^c	-18.16	-2.50	1.81
4	4-n-Butoxy-	108 ^c	-21.56	-5.90	-
				-1.67 ^d	-
5	4-Phenoxy-	210 ^c	-23.21	-7.55	-
6	4-Phenyl-	370 ^b -360 ^c	-24.58	-8.92	-
7	4-Formyl-	12.5 ^c	-16.21	-0.55	1.70 ^f
8	4-Acetyl-	21 ^c -20 ^c	-17.44	-1.78	-
9	4-Propanoyl-	48 ^c -44 ^c	-19.44	-3.78	-
				-1.63 ^d	-
10	4-Carboxymethyl-	36 ^c -38 ^c	-18.90	-3.24	1.96
11	4-Carboxyethyl-	70 ^c -68 ^c	-20.45	-4.79	2.47
12	4-Carboxypropyl-	169 ⁱ	-22.67	-7.01	3.04
				-1.88 ^d	-
13	4-Cyano-	16 ^c -14 ^c	-16.67	-1.01	1.60
14	4-Cyanomethyl-	36 ^c	-18.84	-3.18	-
15	4-Nitro-	17 ^c -15 ^c	-16.83	-1.17	1.91
16	2-Carboxamido-	6 ^c	-14.40	1.26	1.28
17	2-Acetamido-	8 ^c	-15.11	0.55	-
18	4-Methylthio-	49 ^c -46 ^c	-19.52	-3.86	-
19	3-Trifluoromethyl-	130 ^c	-22.02	-6.36	2.95
20	2-N-Phenylcarboxamido-	250 ^c	-23.64	-7.98	3.27
21	2-Nitro-4-chloro	44 ^c	-19.33	-	-
22	3-Nitro-4-methyl-	42 ^c -37 ^c	-19.07	-	-
23	2-Chloro-4-bromo-6-Methyl	330 ^c	-24.33	-	-
24	4-Nitro-2,6-diiodo-	2100 ^c	-28.92	-	-
25	3,5-Dimethoxy-	24 ^c	-17.83	-	-
26	2,6-Dimethoxy-4-acetyl-	36 ^c	-18.84	-	-
27	2-Acetamido-4,6-dichloro-5-methyl-	120 ^c	-21.82	-	-
28	1-Naphthol	180 ^b	-22.83	-	2.98
29	2-N-Butylcarboxamido-	2100 ^c	-28.92	-6.09	-
30	2-N-Phenylcarboxamido	3800 ^c	-30.39	-7.56	-

TABLE 6

Standard free energy change for different substituent groups on phenols in various two-phase media

Substituent	$\Delta\mu_t^0$ (kJ mol ⁻¹)		
	SDS	1-Octanol/water	Hydrocarbon/water
Aliphatic -C- (on phenols)	-2.13	-2.63	-3.16 ^a
Aliphatic -C- (on alkanes)	-3.22	-	-3.68 ^b
Aliphatic -C- (on arenes)	-2.64	-2.82	-3.35 ^b
4-Hydroxy	2.60 ^c	4.97	
Hydroxy (on arenes)	1.72	3.81	17.99 ^b
4-Cyano	-1.01	-0.80	5.25 ^a , 7.19 ^d
4-Nitro	-1.17	-2.56	
4-Phenyl	-8.92		-9.53 ^a
4-Fluoro	-1.38 ^e	-1.77	-0.95/-1.37 ^f
4-Chloro	-2.68 ^e	-5.30	-3.59 ^a
4-Bromo	-4.31 ^e	-6.45	-4.51 ^a
4-Iodo	-6.28 ^e	-8.27	-5.02 ^a /-6.22 ^a
4-Thio-(R)	-1.72	-2.05 ^g	
3-Trifluoromethyl	-6.36	-8.50	
2-Carboxamido	1.26	1.03	
2-N-Phenylcarboxamido	-7.98	-10.33	
4-Formyl	-0.55	-1.37/-1.99 ^h	
4-O-(R)	0.67	3.34	5.59 ^a
4-CO-(R)	-0.42	3.25	
4-COO-(R)	-1.26	0.29	

Table 7. - Extraction Efficiency as a Function of Experimental Parameters for Iron(III)-PAS-C₇

pH	% E	PAS-C ₇ , M	% E	Triton X100/ BL 4.2, % w/v	% E
2.00	39.0	5×10^{-4}	80.0	0.50:0.50	77.6
2.65	74.5	1×10^{-3}	87.5	0.75:0.75	93.6
3.10	88.4	1.5×10^{-3}	92.0	1.00:1.00	93.7
3.50	93.7	2×10^{-3}	93.7	1.50:1.50	94.0
3.75	94.3				

TABLE 8 : Rate constants^a for formation and dissociation of iron(III) monocomplexes with PAS-C₂ and PAS-C₄

	PAS-C ₂	PAS-C ₄
$10^{-3} (k_2 + k_3 K_{OH,w} / K_{a,w}), \text{ dm}^3 \text{ mol}^{-1} \text{ s}^{-1}$	12.9 ± 0.4	8.2 ± 0.3
$10^{-3} k_3^b, \text{ dm}^3 \text{ mol}^{-1} \text{ s}^{-1}$	4.4 ± 0.1	3.6 ± 0.1
$10^{-2} k_4 K_{OH,w}, \text{ s}^{-1}$	2.2 ± 0.1	2.2 ± 0.1
$10^{-4} k_4, \text{ dm}^3 \text{ mol}^{-1} \text{ s}^{-1}$	8.0 ± 0.4	8.0 ± 0.4
$k_{-3}, \text{ dm}^3 \text{ mol}^{-1} \text{ s}^{-1}$	2.3 ± 0.5	1.9 ± 0.1
$10^2 k_{-4}, \text{ s}^{-1}$	5 ± 4	4 ± 1

^a t = 25°C; $\mu = 0.10 \text{ mol dm}^{-3}$. ^b With the assumption that $k_2 \ll k_3 K_{OH,w} / K_{a,w}$ (see text).

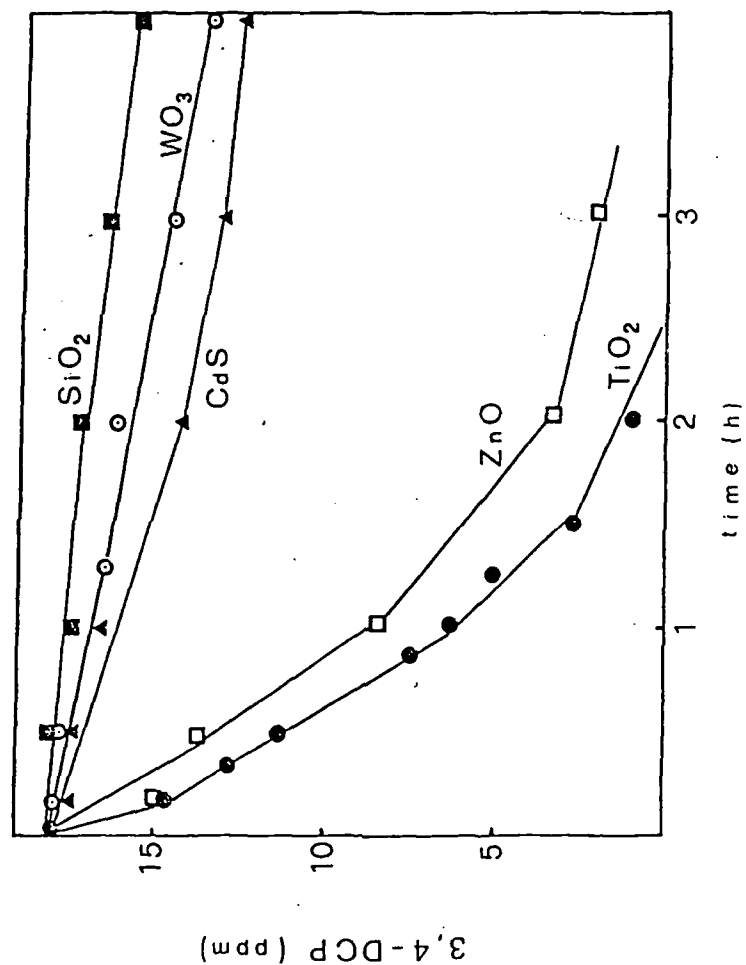


Figure 1. Photodegradation of 3,4-dichlorophenol in the presence of various semiconductor dispersions; wavelength of irradiation > 330 nm; initial 3,4-DCP concentration 18 ppm; O₂ present; initial pH 3.0; unbuffered aqueous solutions; concentration of catalyst, 2.0 g/l.

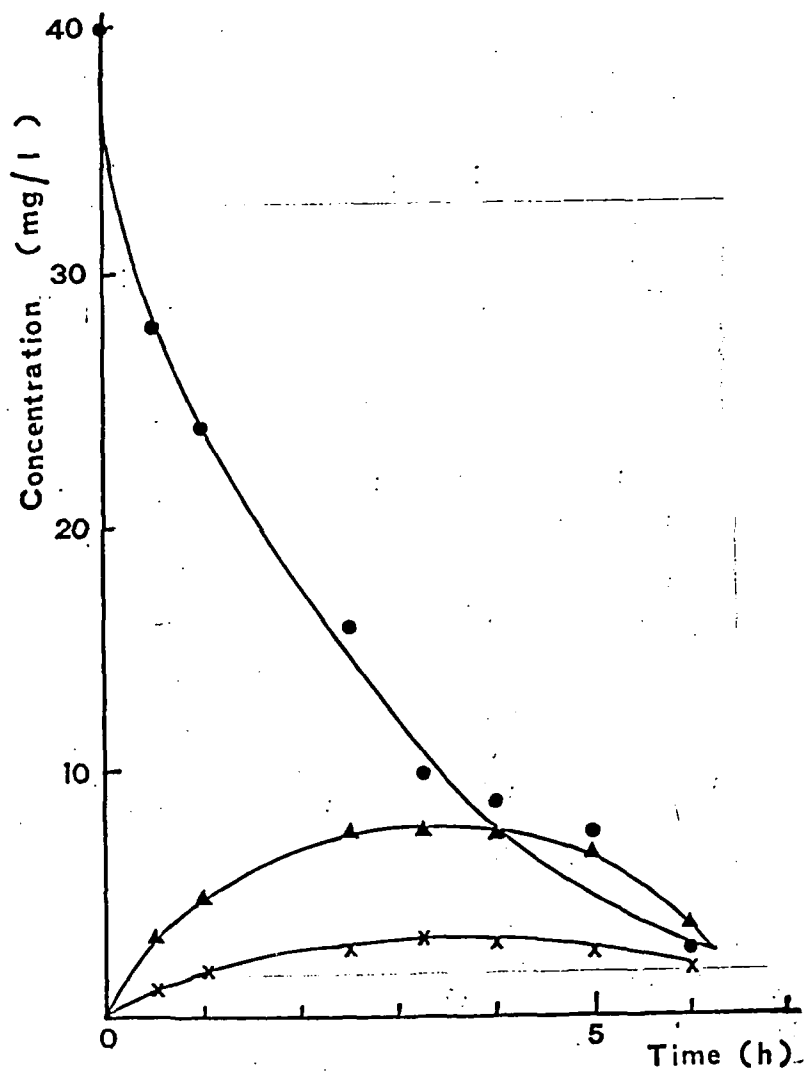


Figure 2 Results of phenol degradation and intermediate formation in the presence of TiO_2 (2 g/l); phenol concentration 40 mg/l; Xenon lamp power 150 W;
 (●) phenol; (X) quinol; (▲) catechol

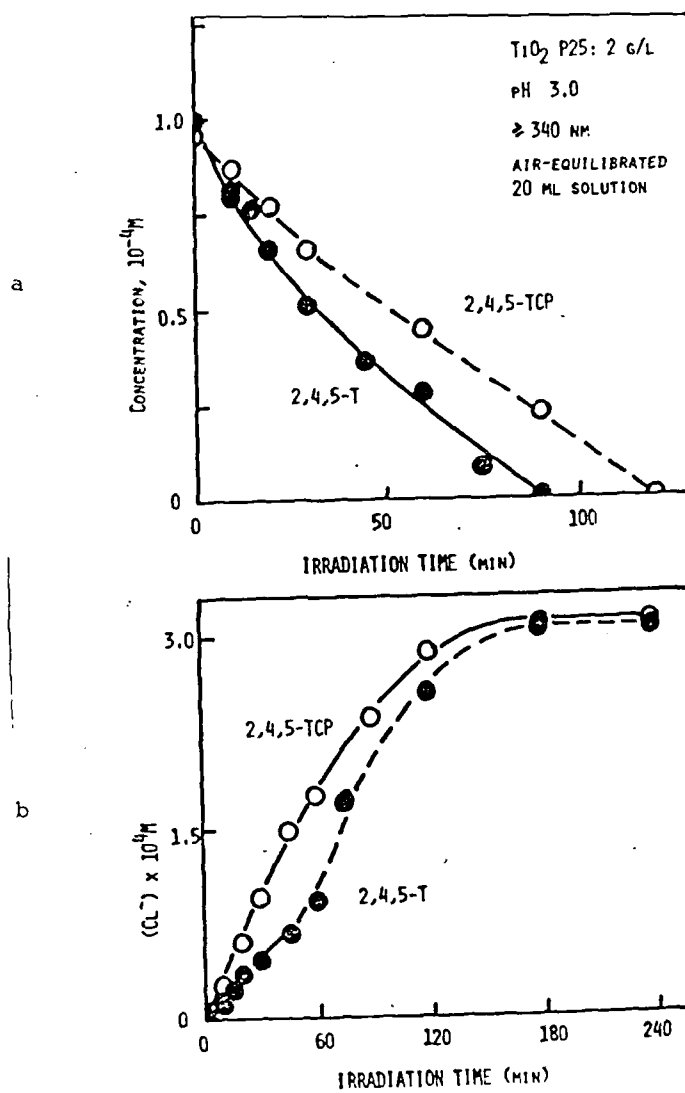


Figure 3 (a) Plot showing the relative decomposition of 2,4,5-T and 2,4,5-TCP as a function of irradiation time
 (b) Plot showing the formation of stoichiometric quantities of chloride ions as a function of irradiation time

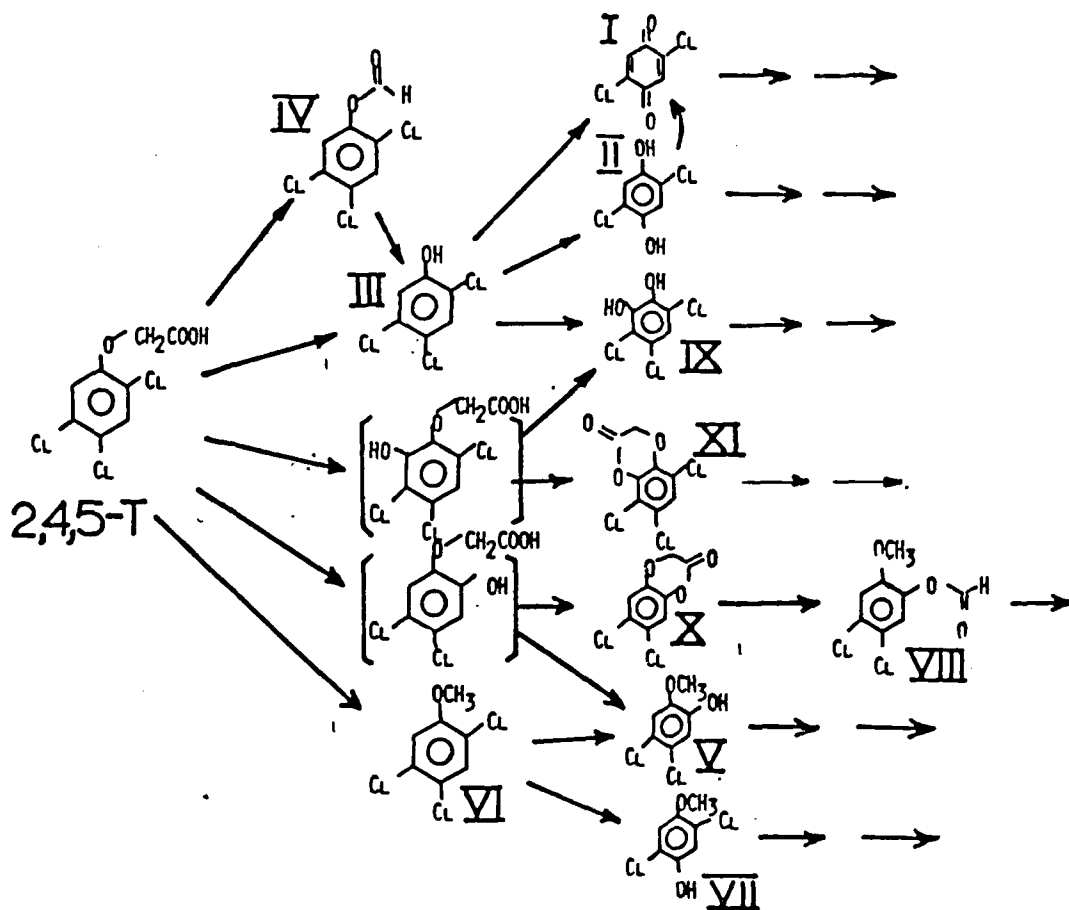


Figure 4 Plausible photodegradation pathway of 2,4,5-T in the presence of TiO_2 under simulated sunlight irradiation conditions.

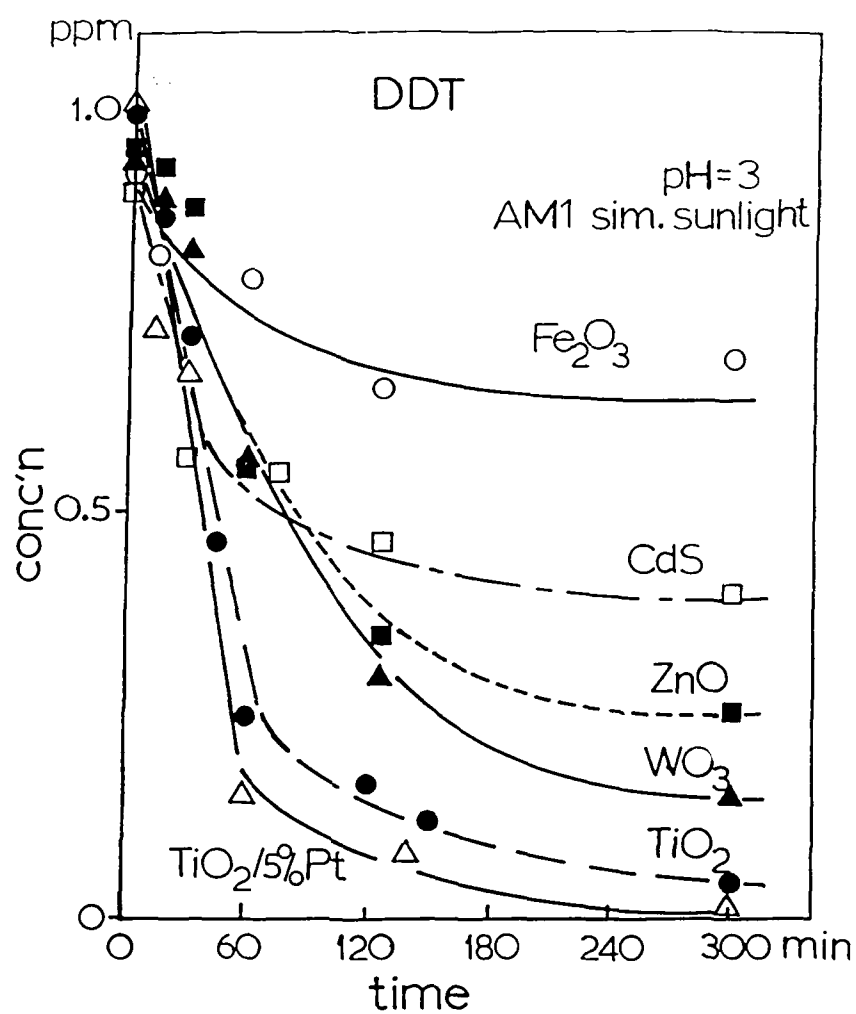


Fig 5 . Plots illustrating the photodegradation of DDT at pH 3 as a function of irradiation time for several semiconductor particulates.

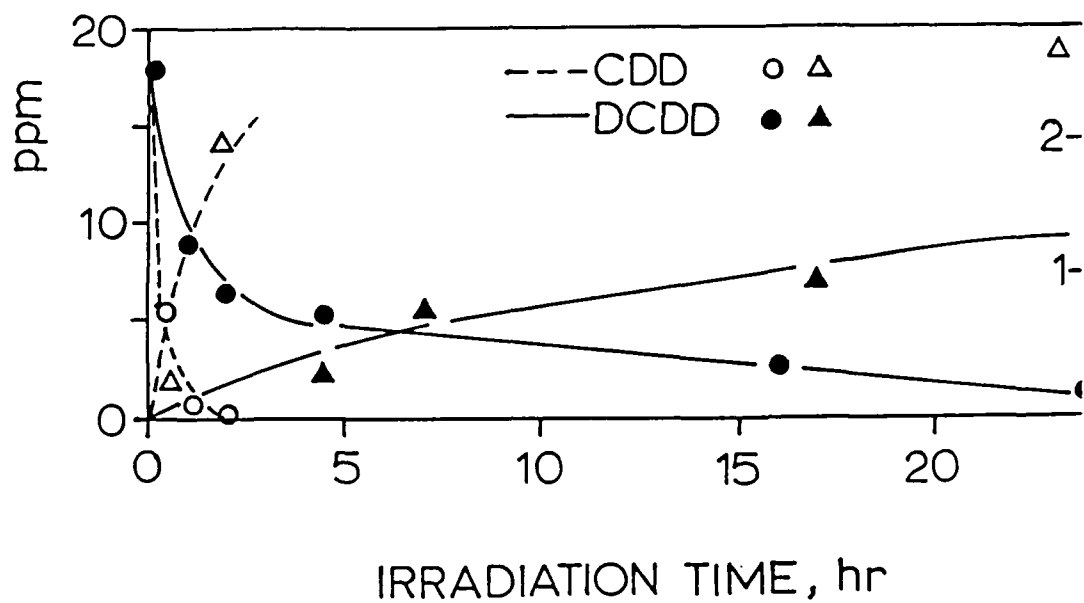


Figure 6 - Concentration versus irradiation time plots in the photodegradation of 2-CDD and 2,7-DCDD; pH 3;

$\text{TiO}_2 = 4 \text{ g/L}$.

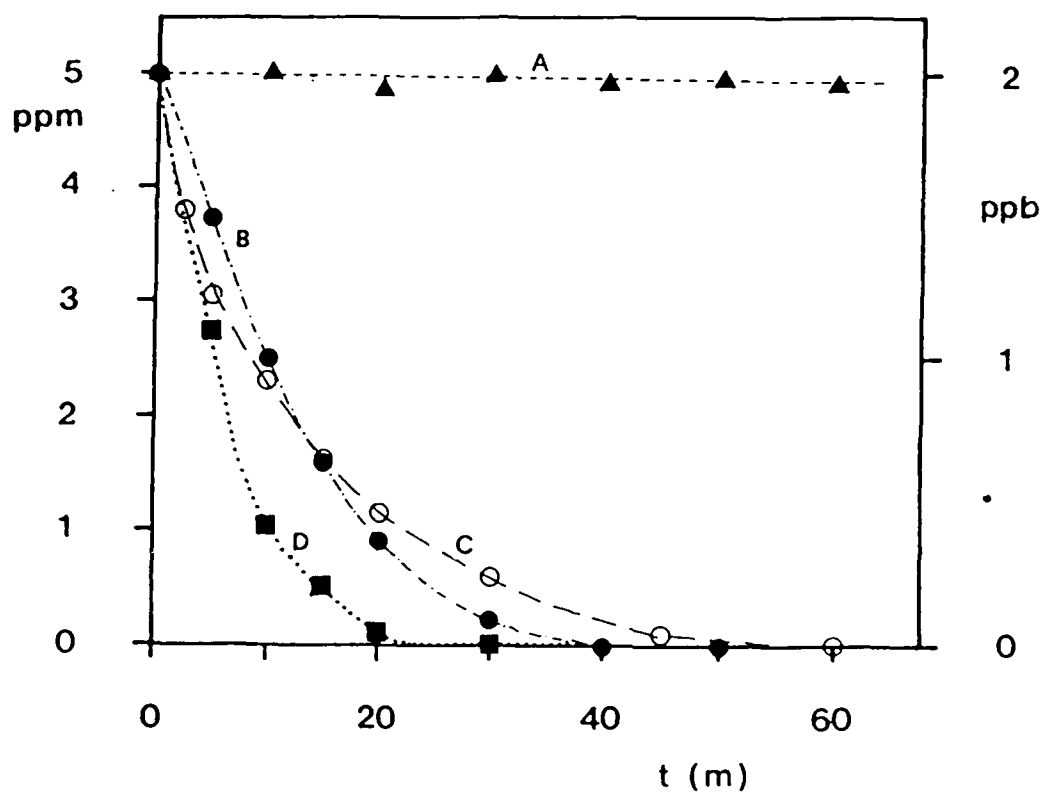


Fig. 7 Plots illustrating the photodegradation of atrazine as a function of irradiation time (Solarbox, $\lambda \geq 340$ nm; unless differently stated): curve A (left scale) : no TiO_2 present - curve B (left scale): 0.1 g/l TiO_2 - curve C (left scale) : 0.1 g/l TiO_2 ; solar exposure (Turin, May 13, 1987, 4-6 p.m.) - curve D (right scale) : 0.1 g/l TiO_2

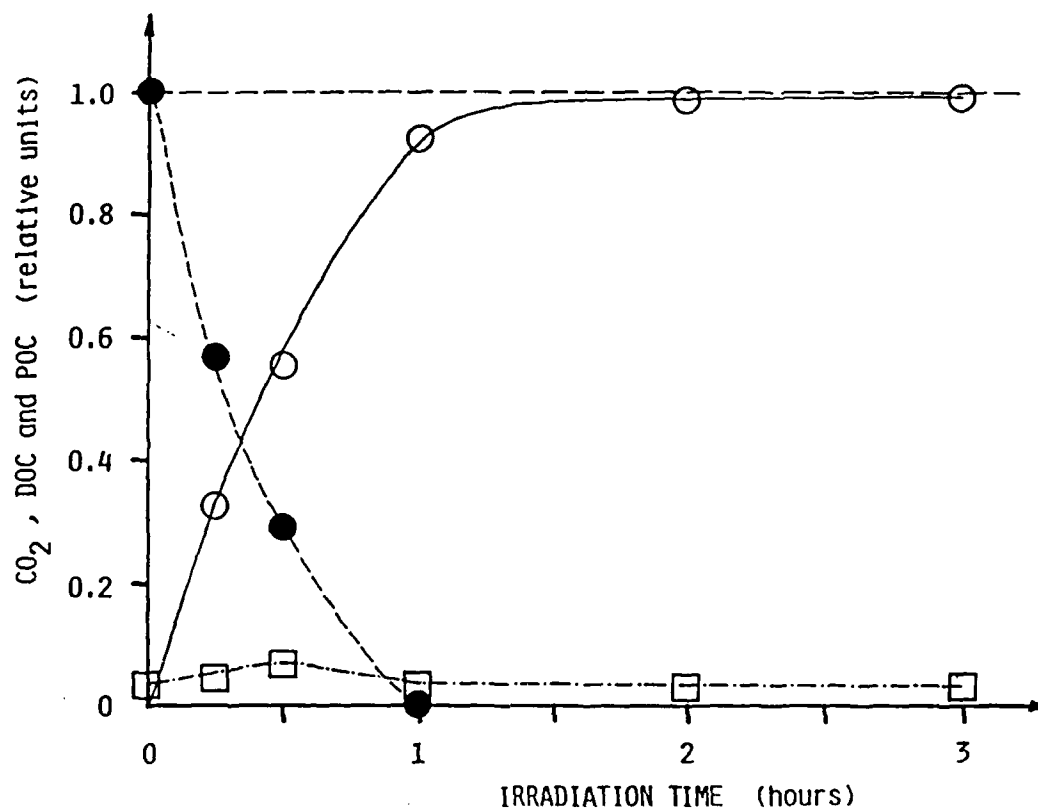


Fig 8

CO_2 (○) evolution, DOC (●) and POC (□) variation as a function of irradiation time for EE. Units are relative to the stoichiometric value: for CO_2 , expected from eq.1; for DOC and POC, relative to total carbon. EE initial concentration 100 ppm; TiO_2 2 gL^{-1} .

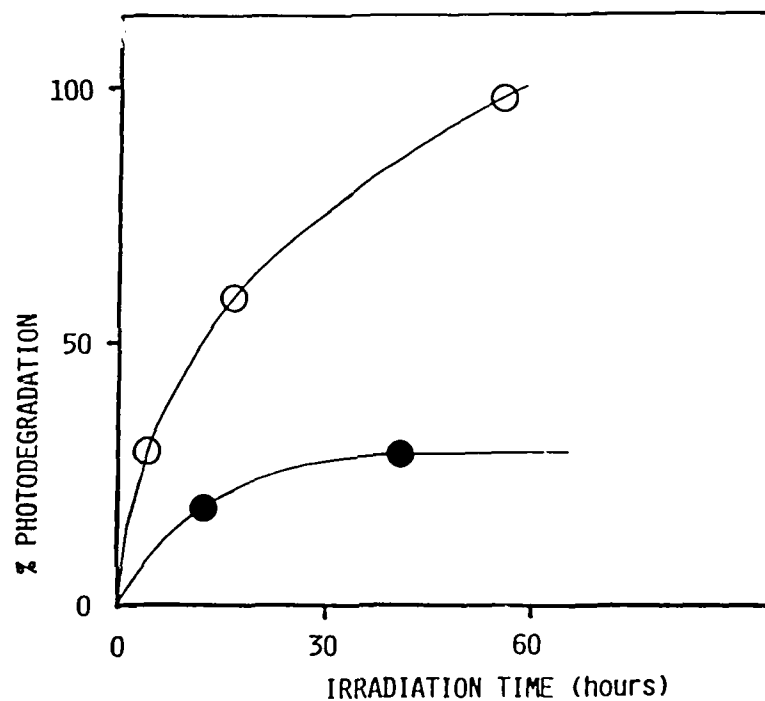


Fig. 9. —

Photocatalytic degradation of BE with organic conducting polymer. Spontaneous photodegradation

(●) and over 30% iodine doped PPA membrane, 8.6 cm² surface area (○). BE initial concentration 2.10^{-3} M, volume 50 mL, spontaneous pH 6.3, irradiation with a 40 watts lamp. Per cent values reported on each curve are corresponding to the highest photodegradation value.

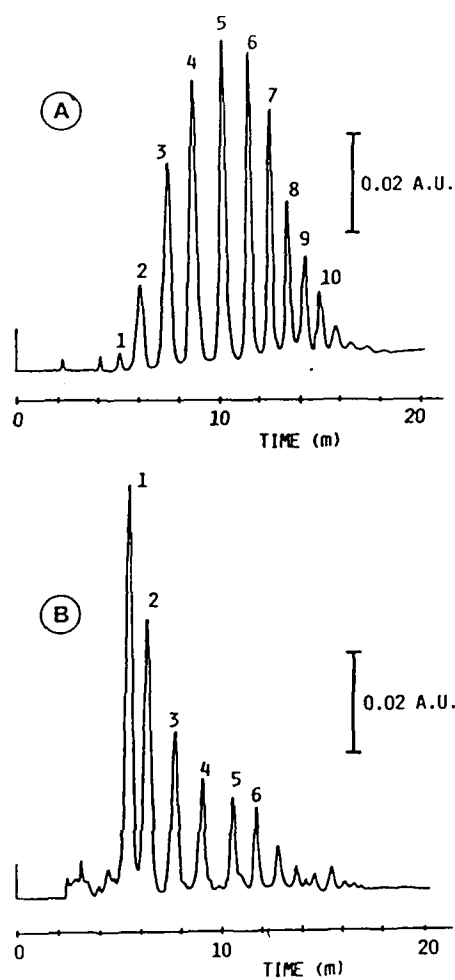


FIGURE 10. Chromatograms before (A) and after 10 minutes of irradiation (B) for IGEPAL CO-520 (6.2×10^{-4} M). TiO_2 , 2 g L^{-1} . Numbers in figure over each peak represent the number of oxyethylene units.

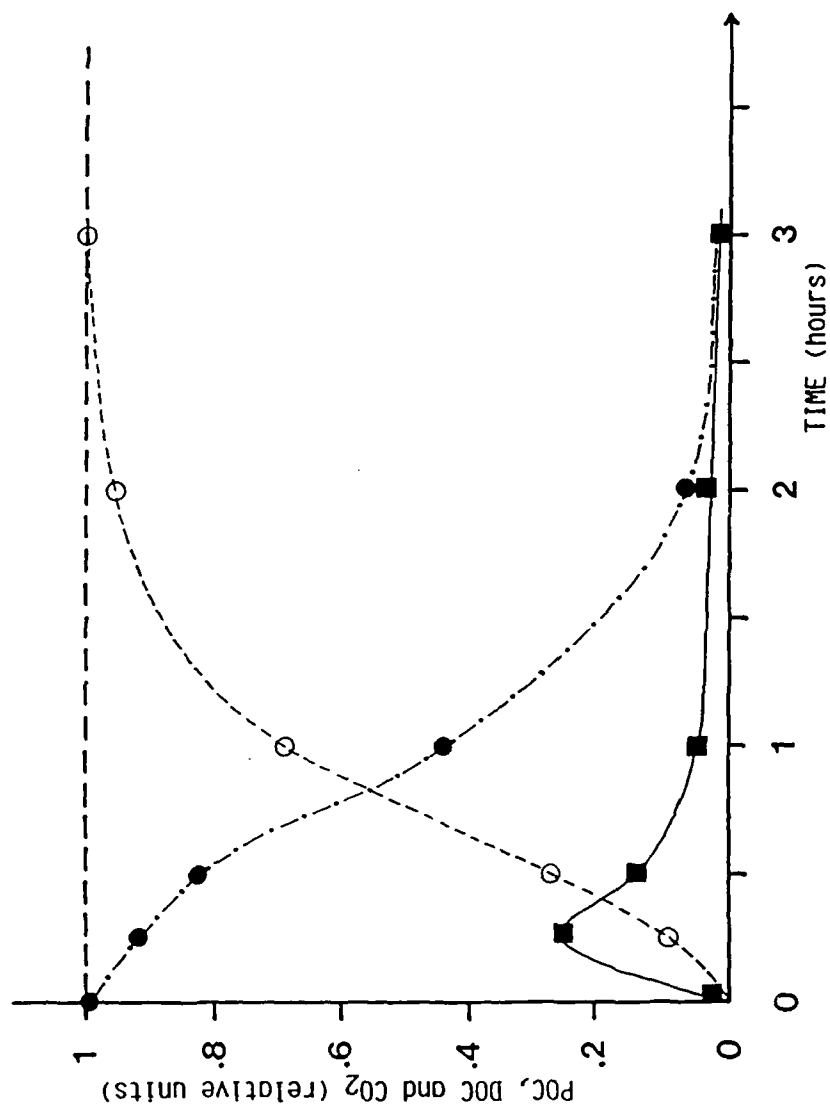


FIGURE 11. CO₂ (O) evolution, DOC (●) and POC (■) variation as a function of irradiation time for IGEPAI CO-720. Units are relative to the stoichiometric value: for CO₂, expected from eq.1; for DOC and POC relative to total carbon. Experimental conditions as in Fig.1 .

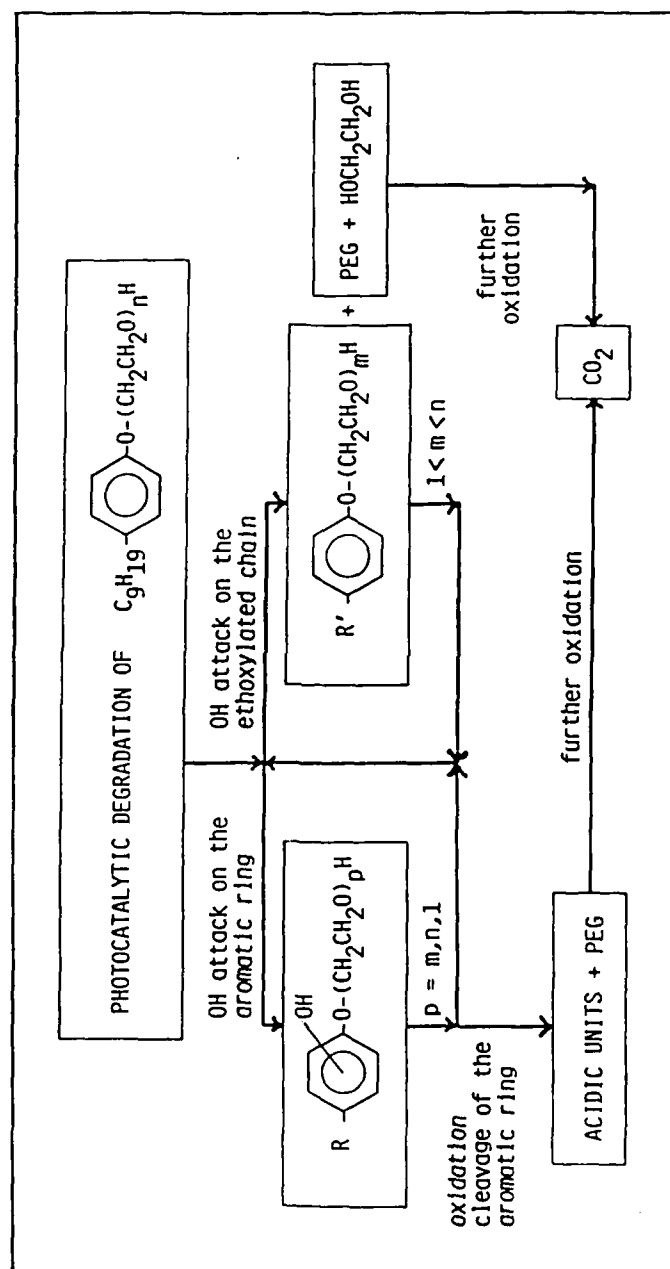
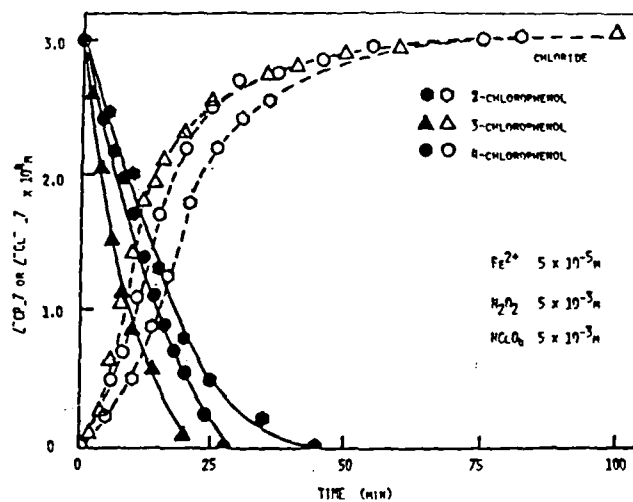


FIGURE 12. Photodegradation routes for NPE's.

Degradation of the aliphatic chain is omitted for clarity.

5



6

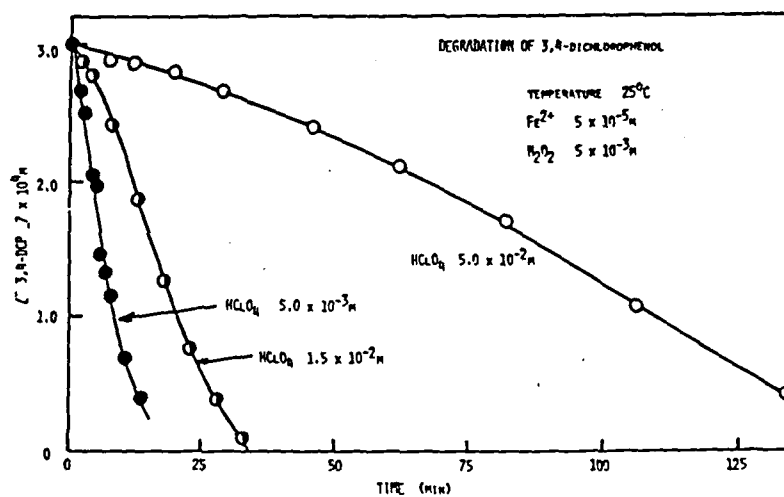


Figure 13 Degradation of monochlorophenols by Fenton's reagent and concomitant appearance of free chloride ions.

Figure 14 Disappearance of 3,4-DCP as a function of time at different HClO_4 concentrations.

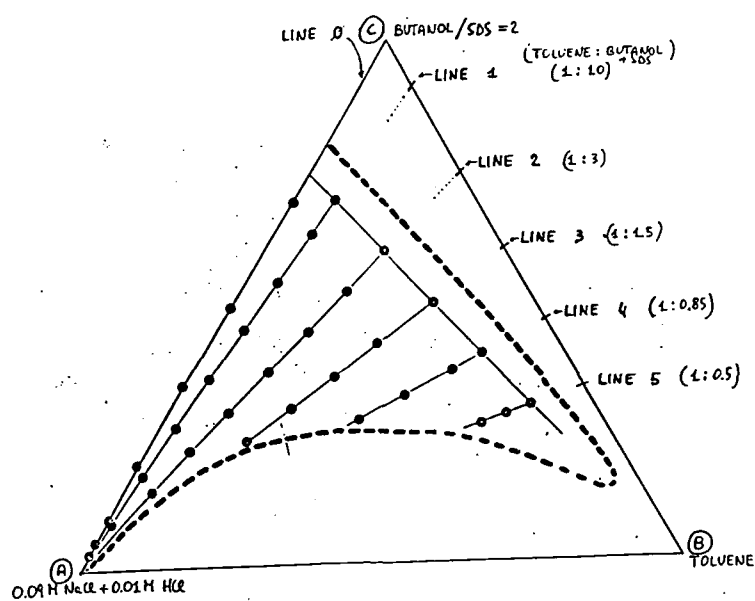


Figure 15 Pseudoternary phase diagram of the system water (0.09 M NaCl + 0.01 M HCl) - toluene - (1-butanol:SDS = 2:1), showing the single-phase at 25 C. The straight lines represent the dilution lines by water and the points the microemulsion compositions at which the kinetic runs were performed

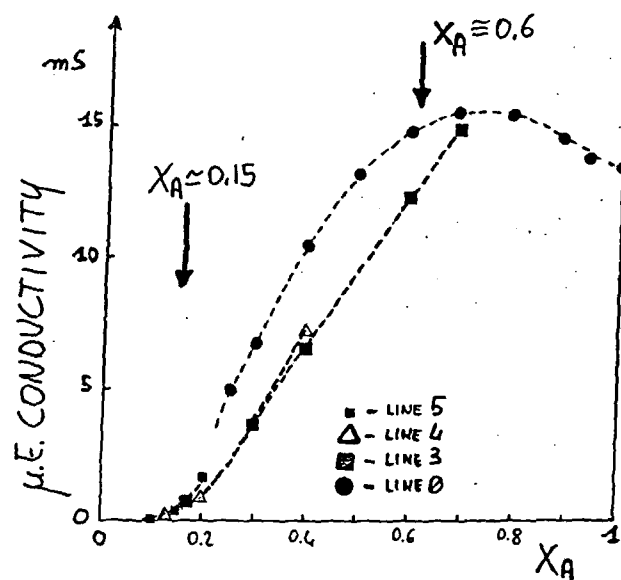


Figure 16 Conductance of a series of microemulsions, according to the lines shown in Fig. 7

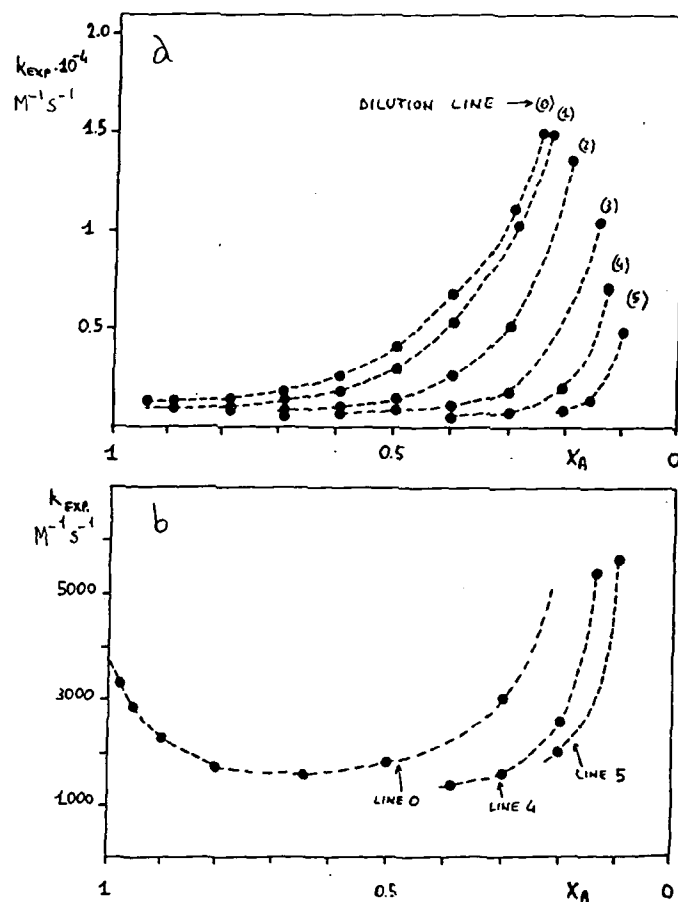


Figure 17 Experimental rate constants for the oxidation of catechols by IrCl_6^{2-} in microemulsions (for the dilution lines see Fig. 7)
 (a) di-*t*-butylcatechol (b) catechol

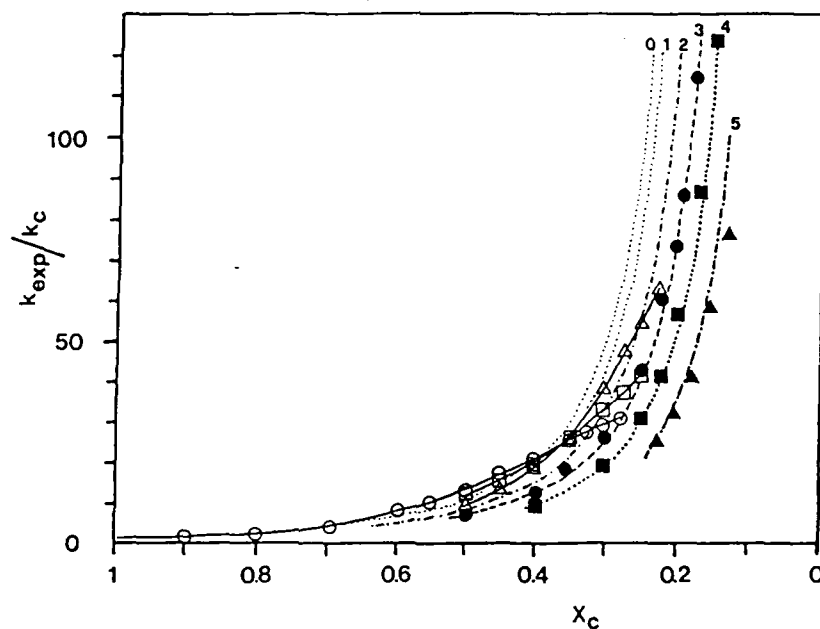


FIG.48: Experimental (points) and calculated (dashed and dotted lines) rate constants in microemulsion for dilution lines 0-5, versus the aqueous weight fraction X_c . Dilution line 0 = (\circ), dilution line 1 = (\square), dilution line 2 = (\triangle), dilution line 3 = (\bullet), dilution line 4 = (\blacksquare), dilution line 5 = (\blacktriangle). The fit curves are calculated with the following parameters in eq.(24): $P_{wi}^A=0.15$, $P_{wo}^A=0$, $P_{wi}^B=0.02$, $P_{wo}^B=0$, where $A=IrCl_6^{3-}$ and $B=CoW_{12}O_{40}^{5-}$.

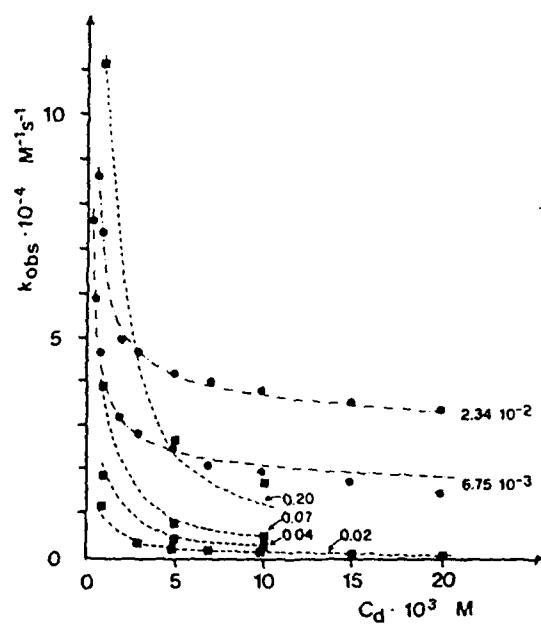


Figure 19. Second-order rate constant ($\text{L mol}^{-1} \text{s}^{-1}$) observed as function of the surfactant concentration at fixed added salt: (●) Na_2SO_4 ; (■) NaCl . Concentrations of the added salt are indicated. Dashed lines refer to the behavior calculated according to eq 18.

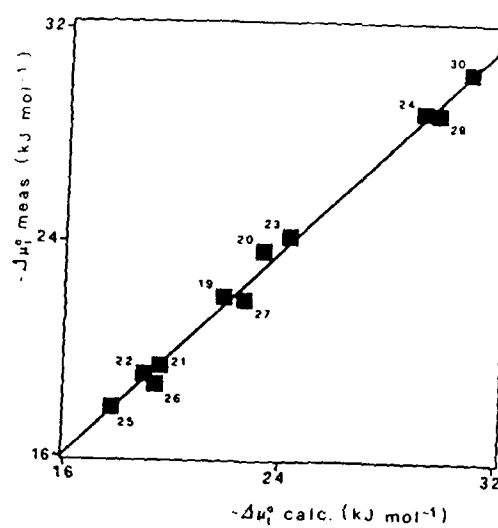


Fig. 20

Comparison between calculated and measured
free energies of transfer of polysubstituted
phenols (correlation coefficient 0.996)

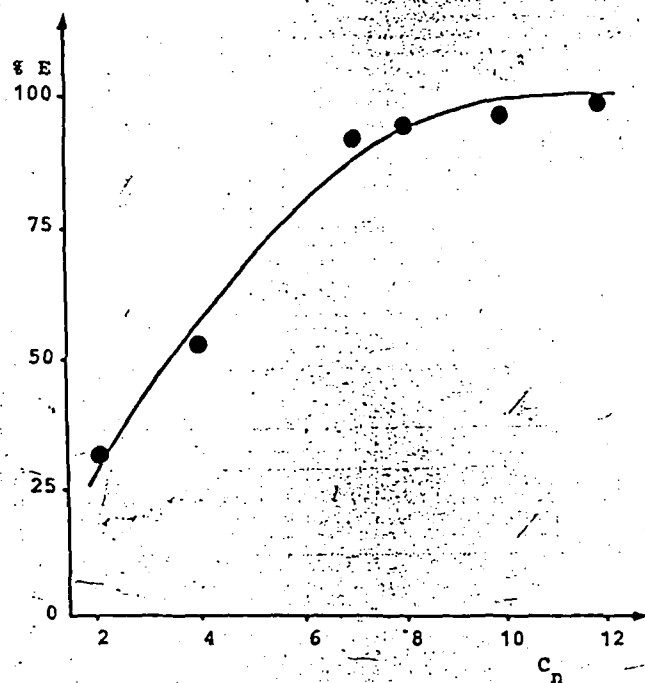


Figure 21 Plot of the percent extraction of iron (III) as a function of ligand alkyl chain length.

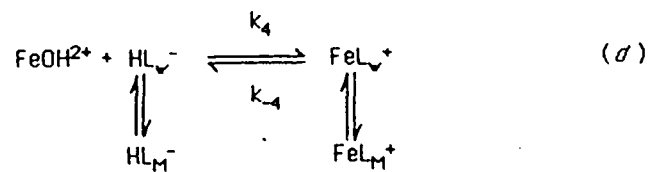
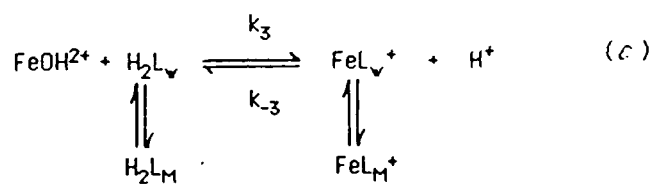
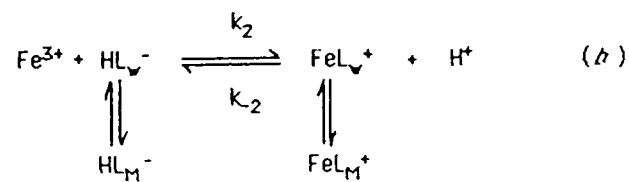
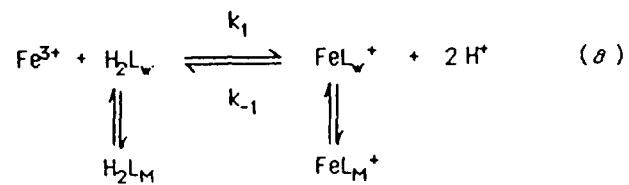


Fig. 22

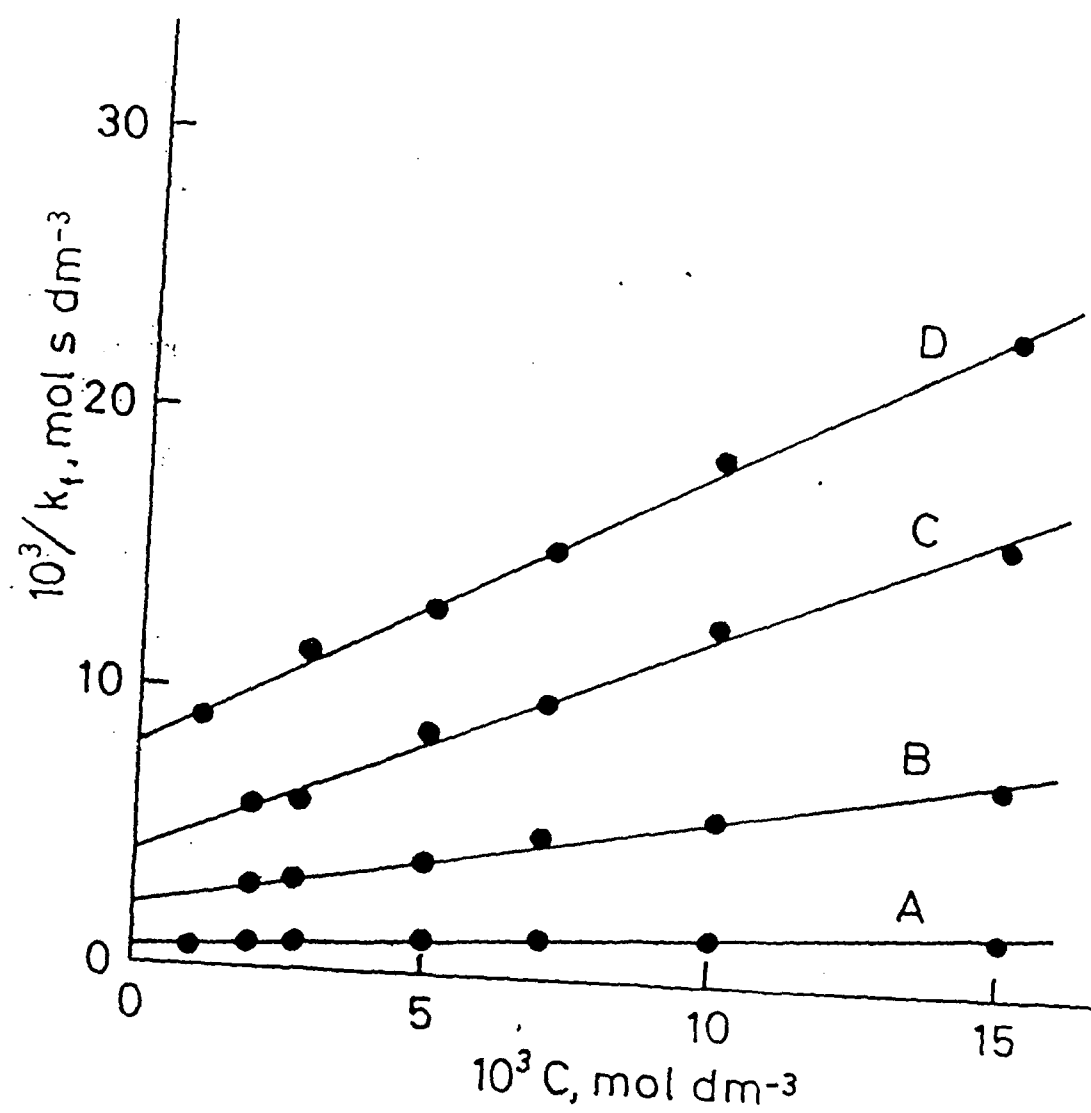


Fig 23
Plots of $1/k_1$ against C for ligand PAS- C_2 at $[H^+] = 1.67 \times 10^{-2}$
(A), 3.87×10^{-2} (B), 6.06×10^{-2} (C), and $11.3 \times 10^{-2} \text{ mol dm}^{-3}$
(D).

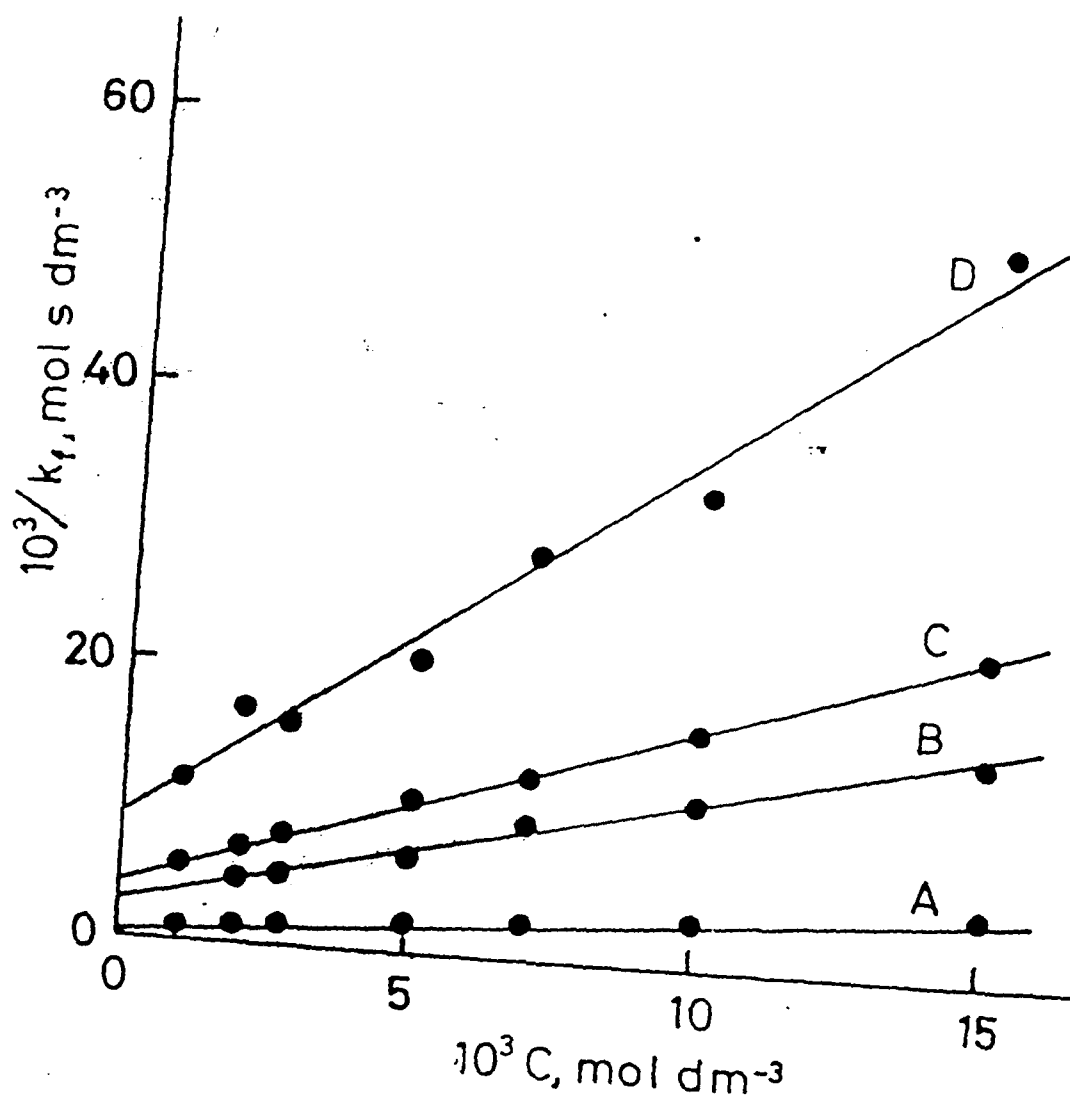


Fig. 24
Plots of $1/k_f$ against C for ligand PAS-C₄ at $[H^+] = 1.74 \times 10^{-2}$
(A), 4.38×10^{-2} (B), 6.42×10^{-2} (C), and 11.3×10^{-2} mol dm⁻³
(D).